ACS OMEGA

http://pubs.acs.org/journal/acsodf

Article

Potential Mechanisms of Imidacloprid-Induced Neurotoxicity in Adult Rats with Attempts on Protection Using *Origanum majorana* L. Oil/Extract: *In Vivo* and *In Silico* Studies

Eman I. Hassanen, Marwa Y. Issa, Neven H. Hassan, Marwa A. Ibrahim, Iten M. Fawzy, Sherif Ashraf Fahmy,* and Sally Mehanna

Cite This: *ACS Omega* 2023, 8, 18491−18508

Read Online

ACCESS | Metrics & More | Article Recommendations

ABSTRACT: Imidacloprid (IMI) insecticide is rapidly metabolized in mammals and contributes to neurotoxicity via the blocking of nicotinic acetylcholine receptors, as in insects. *Origanum majorana* retains its great antioxidant potential in both fresh and dry forms. No data is available on the neuroprotective effect of this plant in laboratory animals. In this context, aerial parts of *O. majorana* were used to prepare the essential oil (OMO) and methanol extract (OME). The potential neuroprotective impact of both OMO and OME against IMI-induced neurotoxicity in rats was explored. Forty-two rats were divided into 6 groups, with 7 rats in each one. Rats were daily administered the oral treatments: normal saline, OMO, OME, IMI, IMI + OMO, and IMI + OME. Our results revealed the identification of 55 components in *O. majorana* essential oil, most belonging to the oxygenated and hydrocarbon monoterpenoid group. Moreover, 37 constituents were identified in the methanol extract, mostly phenolics. The potent neurotoxic effect of IMI on rats was confirmed by neurobehavioral and neuropathological alterations and a reduction of both acetylcholine esterase (AchE) activity and dopamine (DA), serotonin (5HT), and γ-aminobutyric acid (GABA) levels in the brain. Exposure of rats to IMI elevates the malondialdehyde (MDA) levels and reduces the antioxidant capacity. IMI could upregulate the transcription levels of nuclear factor-κB (NF-κB), interleukin-1 β (IL-1β), and tumor necrosis factor (TNF-α) genes and express strong caspase-3 and inducible nitric oxide synthase (iNOS) immunostaining in most examined brain areas. On the other hand, rats coadministered OMO or OME with IMI showed a marked improvement in all of the studied toxicological parameters. In conclusion, cotreatment of *O. majorana* extracts with IMI can protect against IMI neurotoxicity via their potent antioxidant, anti-inflammatory, and anti-apoptotic effects. Thus, we recommend a daily intake of *O. majorana* to protect against insecticide's oxidative stress-mediated neuroinflammatory stress and apoptosis. The molecular docking study of linalool, rosmarinic acid, γ-terpene, and terpene-4-ol justify the observed normalization of the elevated iNOS and TNF-α levels induced after exposure to IMI.

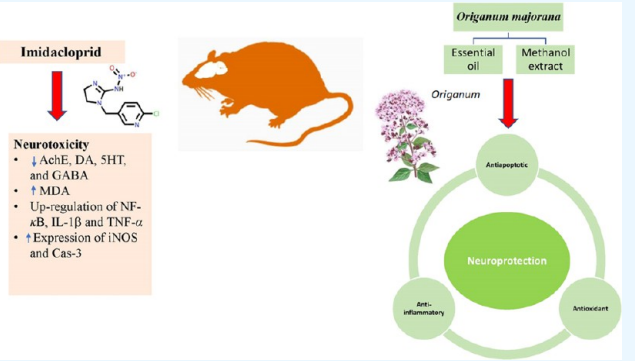

1. INTRODUCTION

Neonicotinoids constitute a major class of extremely effective insecticides used to protect cotton, cereal, tea, and vegetable crops from piercing−sucking insects, as well as for flea control in cats and dogs, and to control cockroaches, termites, turf pests, and ants in lawns, gardens, and homes. The most well-known neonicotinoid is imidacloprid [IMI, 1-(6-chloro-3-pyridylmethyl)-*N*-nitroimidazolidin-2-ylideneamine], an effective neurotoxic pesticide that acts as a selective agonist at the nicotinic acetylcholine receptors (nAChRs) in insects. It was initially introduced in the market in 1991 for veterinary usage and crop protection.[1] It has become one of the most used pesticides worldwide, accounting for 41.5 percent of the total neonicotinoid market due to its low toxicity, great systemic characteristics, extensive insecticidal usage, and highly specific insecticidal activity.[2]

Although neonicotinoids are thought to have minimal mammalian toxicity, several studies suggested that prolonged imidacloprid exposure can induce various health problems in animals and humans.[3−5] To date, previous studies have been performed at the animal model, human population, and cellular

Received: December 31, 2022
Accepted: April 19, 2023
Published: May 17, 2023

levels, and they have revealed a variety of biological−chemical reactions that may cause imidacloprid's negative health impacts. Moreover, in laboratory animals, IMI administration may result in neurotoxicity, mutagenicity, teratogenicity, immunotoxicity, reproductive toxicity, and infertility. In addition, it induces nephrotoxicity and hepatotoxicity.[6] IMI also may serve as an endocrine disruptor by interfering with steroid hormone synthesis.[7]

Plant-based medications may be useful in reducing oxidative stress caused by environmental neurotoxicants. Consumption of natural antioxidants derived from plants has been shown to reduce the levels of numerous oxidative stress and/or proinflammatory biomarkers.[8] In the category of natural plant medicines, oregano, one of the active herbs and spices, comprises a wide range of compounds with potent pharmacological and biological effects.[9,10] It is distributed throughout the world but is most prevalent in the Mediterranean,[11−13] North Africa, and Eurasia.[14] Both fresh and dry forms of oregano retain its great antioxidant potential.[15] Oregano leaves, the dried herb, and its essential oil have been used to treat indigestion, rheumatoid arthritis, and respiratory diseases.[9] Hydrocarbons or oxygenated monoterpenes, which are the principal components of oregano's essential oil, are considered to be responsible for its antibacterial, antioxidant, and anti-inflammatory characteristics.[16] Lately, oregano has received significant interest due to its various pharmacological activities, including its potential protection against neurodegenerative disorders and neurotoxicity. Therefore, oregano was chosen to counteract the neurotoxic effect of IMI in the current study as a neuroprotective agent against neuroinflammation and oxidative stress with its associated dysregulated neurotransmitter as well as neurobehavioral toxicity induced by IMI.

This study aims to evaluate the potentially hazardous effects of IMI on different brain areas in rats and uncover the exact mechanistic molecular pathway involved in counteracting these detrimental effects via administering both *Origanum majorana* L. oil and its methanol extract. Additionally, we compare their phytochemical constituents and proposed neuroprotective capability *in vivo* employing a rat animal model and in silico using molecular docking.

2. MATERIALS AND METHODS

2.1. Chemicals. The commercial formulation of imidacloprid was procured from Kafr El-Zayat Pesticides and Chemicals Company (Kafr El-Zayat, Gharbia, Egypt). The concentration of active ingredients of imidacloprid is 70%; its IUPAC name is (NE)-*N*-[1-[(6-chloropyridin-3-yl)methyl]-imidazolidine-2-ylidene] nitroamide and the chemical formula $C_9H_{10}ClN_5O_2$. The formulation was provided in the form of wettable powder, which was freshly dissolved in deionized water prior to administration.

Analytical-grade chemicals were used in this research; HPLC grade formic acid and methanol (Sigma-Aldrich) for liquid chromatography−mass spectrometry (LCMS) (LiChropur). Double-deionized water with a conductivity of less than 18.0 MΩ was acquired from a Milli-Q system (Merck KGaA, Darmstadt, Germany).

2.2. Plant Collection and Extraction. *O. majorana* L. (aerial parts) were collected from the Experimental Station of Medicinal Plants, Faculty of Pharmacy, Cairo University, Giza, Egypt, on May 2020. The plant was identified and verified at the Faculty of Science Herbarium, Cairo University. The plant was dried in the shade and then ground. Clevenger's apparatus was used for the hydrodistillation of small pieces of sliced aerial parts of oregano to prepare the oregano oil. The distillation lasted for 3 h; then, the collected oil was dried using anhydrous sodium sulfate. For the preparation of the oregano extract, 1 kg of the ground powder was successively extracted till exhaustion with 80% methanol to give 178 g of a dark green residue. The samples were stored at −20 °C in a freezer till analysis and further biological activity evaluation.

2.3. Analysis of Oregano Samples. *2.3.1. GC/MS Analysis of the Essential Oil.* Shimadzu GCMS-QP2010 (Kyoto, Japan) containing an Rtx-5MS fused bonded column (30 m × 0.25 mm i.d. × 0.25 μm film thickness) (Restek) and a split−splitless injector was employed. The injector temperature was laid at 250 °C. A successive ramp temperature program was used for the analysis of volatiles. The beginning column temperature was kept at 45 °C for 2 min., ramped at a rate of 5 °C/min. to 300 °C, and then retained at 300 °C for 5 min. The carrier gas helium was used with a flow rate of 1.41 mL/min. A quadrupole mass spectrometer was activated in EI mode at 70 eV with an ion source temperature of 200 °C and an interface temperature of 280 °C. A scan range of m/z 40−500 was applied. Diluted specimens (1% v/v) were injected in split mode (split ratio 1: 15). Three repeats were analyzed for the essential oil.[17]

2.3.2. Ultraperformance Liquid Chromatography−Mass Spectrometry (UPLC-MS)/MS Identification of the Oregano Methanol Extract. The sample was dissolved using HPLC grade methanol at a concentration of 100 μg/mL. Then, it was filtered with a membrane disc filter (0.2 μm) before applying it to LCMS analysis using a UPLC/ESI-MS, ACQUITY UPLC System—Waters Corporation. The system was equipped with an ACQUITY UPLC-BEH C18 (1.7 μm − 2.1 × 50 mm) column, and the sample was injected at 10 μL. The solvent system consisted of (A) water comprising 0.1% formic acid and (B) methanol comprising 0.1% formic acid. Ramped mobile phase elution was programed starting with 90% A: 10% B that was maintained for 2 min, then reached 70% A after 5 min, 30% A after 15 min, 10% A after 22 min, and kept for 3 min and then reached 100% B after 26 min and was upheld for 3 min and resumed to the first composition after 32 min., and the flow rate: 0.2 mL/min. The analysis was conducted in negative ionization mode with an XEVO TQD triple quadrupole, Waters Corporation, Milford, MA01757 U.S.A, mass spectrometer. The mass spectrometer was operated with a cone voltage of 30 eV, capillary voltage of 3 kV, source temperature of 150 °C, desolvation temperature of 440 °C, desolvation gas flow rate of 900 L/h, and cone gas flow rate of 50 L/h. The mass spectral range in the electrospray ion (ESI) was at m/z 100−1000. Masslynx 4.1 software was used for peak and spectra processing, and metabolites were tentatively identified by comparison of their retention times (R_t) and mass spectra with their counterparts reported in databases and the literature.[18]

2.4. Animals and Experimental Design. Forty-two adult male Wistar rats, weighing 170−200 g, were used in this study. The animals were obtained from the Department of Veterinary Hygiene and Management's Animal House. They were maintained in plastic cages, fed a commercially balanced diet, and given free access to water. Their health status was checked regularly and adapted to the laboratory environment for 14 days before use. The experimental design was accepted by Cairo University's Institutional Animal Care and Use

https://doi.org/10.1021/acsomega.2c08295
ACS Omega 2023, 8, 18491−18508

Table 1. Primer Sets of the Assessed Genes[a]

genes	sense	antisense	amplicon	accession no.
IL-1β	TTGAGTCTGCACAGTTCCCC	GTCCTGGGGAAGGCATTAGG	161	NM_031512.2
TNF-α	ACACACGAGACGCTGAAGTA	GGAACAGTCTGGGAAGCTCT	235	NM_012675.3
NF-κB	ACCTGGAGCAAGCCATTAGC	AGTTCCGGTTTACTCGGCAG	234	NM_199267.2
ACTB	CCGCGAGTACAACCTTCTTG	CAGTTGGTGACAATGCCGTG	297	NM_031144.3

[a]Abbreviations: IL-1β, interleukin-1β; TNF-α, tumor necrosis factor α; NF-κB, nuclear factor κB protein; and ACTB, actin biotin housekeeping gene.

Committee (IACUC) (IACUC protocol number: Vet Cu 2009 2022489). Our experiment complies with the National Institutes of Health (NIH) guidelines.

Male rats were randomly assigned into six groups (n = 7) and were provided IMI and/or oregano samples via oral intake every day for 60 days. Group 1 was given normal saline and served as the control group. Groups 2 and 3 were given 200 mg/kg bwt/day of *O. majorana* oil (OMO) or methanol extract (OME), respectively. The fourth group received 45 mg/kg bwt/day IMI. Groups 5 and 6 were given cotreatments of IMI (45 mg/kg bwt/day) and 200 mg/kg bwt/day from OMO or OME, respectively. The imidacloprid dose exemplifying 1/10 LD50 was chosen in accordance with a previous study,[19] and the oregano sample dose was chosen based on former studies.[20]

2.5. Behavioral Parameters. *2.5.1. Open Field Test.* The open field is a commonly used measure for assessing both anxiety-like behavior and locomotion.[21] This test was carried out in a wooden arena measuring 90 × 90 × 25 cm and coated with formica to avoid rat urine absorption. The arena floor was split into 36 squares by black lines (15 × 15 cm). The rat was positioned randomly in a corner of the arena and permitted to confront it freely for 3 min. During the test duration, the time spent immobile, exploratory behavior in the form of squares crossed and rearing against the wall, as well as nonexploratory behavior in the form of fecal boli and urination, were recorded.

2.5.2. Forced Swim Test. The forced swim test is a behavioral test used to assess the antidepressant potency of new compounds as well as experimental manipulations directed at providing or preventing depressive disorder.[22] Rats were placed individually in a cylindrical bowl (20 × 50 cm) filled with water (20 ± 2 °C). The water level (30 cm height) prevents the rat from resting on its tail or climbing out of the cylinder. For a 5 min test, the duration mobility period (represented swimming and climbing) and the immobility period (represented floating) were recorded during the last 4 min.[23]

2.5.3. Spatial Y-Maze Memory Test. The Y-maze memory test is conducted to evaluate spatial learning and short-term memory in rodents.[24] The Y-maze apparatus comprises three arms labeled A, B, and C with 30 cm height, 15 cm width, and 40 cm length. Rats were positioned individually at one of the arm's ends and given 5 min to move freely through the maze. The arm entry sequence was recorded (i.e., ABCABABCACBAB), and the percentage of spontaneous alternation behavior (a measure of short-term spatial memory) was determined as the ratio of actual alternations to all possible alternations.[25]

2.6. Sampling. Following behavioral evaluations, animals were euthanized in order to collect the entire brain. Half of the brain was kept at 80 °C to measure AchE, neurotransmitters, and oxidative stress parameters and to conduct molecular studies. The remaining half was preserved in 10% neutral buffered formalin for histopathology and immunohistochemistry.

2.7. Assessment of Brain AchE Activity and Neurotransmitter Concentration. A known weighed brain sample was homogenized with ice-cooled saline (0.9% NaCl) to prepare a 20% w/v homogenate. The homogenate undergoes centrifugation at 4000 rpm for 5 min. Neurotransmitters and AchE activity in the whole brain tissue aliquot were then determined. The determinations of cholinesterase activity were done, as previously described by Ellman et al.[26] with modification by Gorun et al.[27] The procedure principle is the measurement of the thiocholine formed when acetylcholine is hydrolyzed. At 412 nm, the color was read immediately. Dopamine (DA), serotonin (5HT), and γ-(GEORGE)-aminobutyric acid (GABA) were determined using HPLC. The sample was immediately extracted from the trace elements and lipids using a solid phase extraction Chromabond column NH2 phase, cat. No.730031. Then, samples were directly injected into an AQUA column 150 mm × 5 cm C18, purchased from Phenomenex, under the following conditions: mobile phase 20 mM potassium phosphate, pH 2.5, flow rate 1.5 mL/min, UV 270 nm. After 12 min, dopamine and serotonin were separated. The resulting chromatogram identified each monoamine position and concentration from the sample as compared to that of the standard (Sigma Chemical Co., St. Louis, MO). Then, the concentration of each monoamine was measured as μg/gram brain tissue finally according to Pagel et al.[28] The precolumn PITC derivatization technique was used to evaluate γ-aminobutyric acid (GABA) levels, as illustrated by Heinrikson and Meredith.[29]

2.8. Oxidative Stress Evaluations. Frozen brain tissue samples were homogenized using cold buffer (pH 7.5) and then centrifuged at 4000 rpm for 15 min at 4 °C to obtain the supernatant used for the Redox status assessment. The malondialdehyde (MDA) level, reduced glutathione (GSH) content, and catalase (CAT) activity were assessed following the instruction of the producer kits obtained from Biodiagnostic Co., Egypt.

2.9. Quantitative RT-PCR Analysis of IL-1β, TNF-α, and NF-κB Genes. The RNeasy Mini Kit (Qiagen Cat No./ID: 74104) was used to isolate the T-RNA from the brain tissues. Samples were used for cDNA synthesis at an optical density of A260/A280 = 1.9−2.1. The SuperScript reverse transcriptases (Thermo Scientific) were used to synthesize the first-strand cDNA, according to the manufacturer's instructions. Quantitative real-time PCR was performed using the SYBR Green PCR master mix (Thermo Scientific, Cat number: 4309155) and the ABI Prism StepOnePlus Real-Time PCR System (Applied Biosystems) according to the manufacturer's instructions. The primer sets of the assessed genes were collected in Table 1. The QRT-PCR was programmed as follows: initial denaturation of 10 min at 95 °C followed by 40 cycles of 20 s/95 °C, and 30 s/60 °C. The

https://doi.org/10.1021/acsomega.2c08295
ACS Omega 2023, 8, 18491−18508

(A)

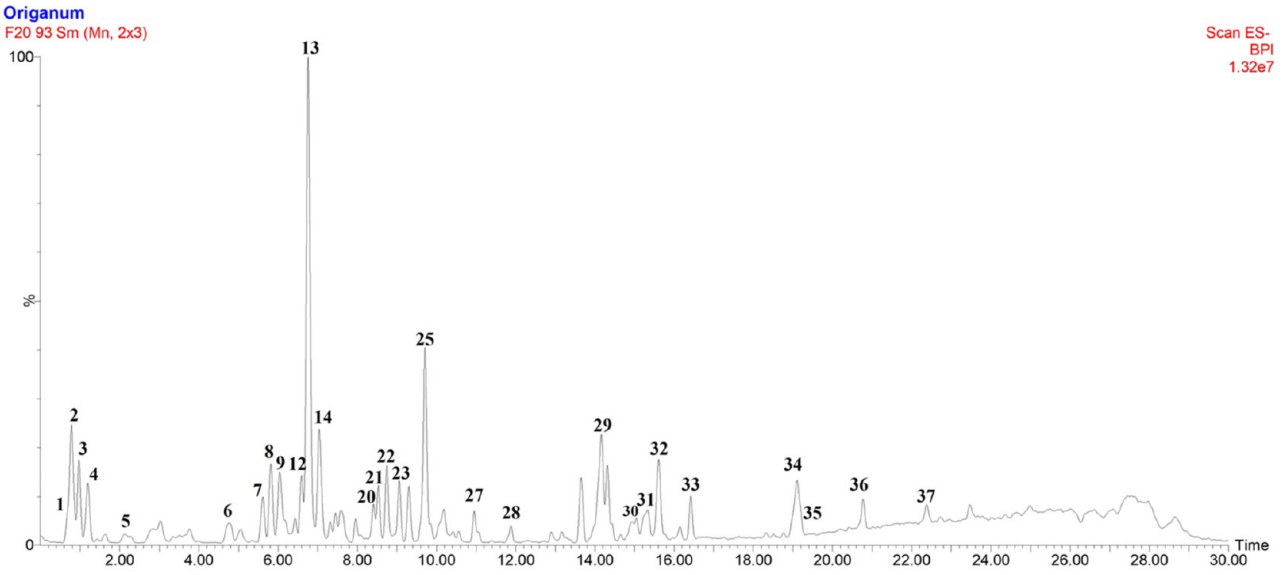

(B)

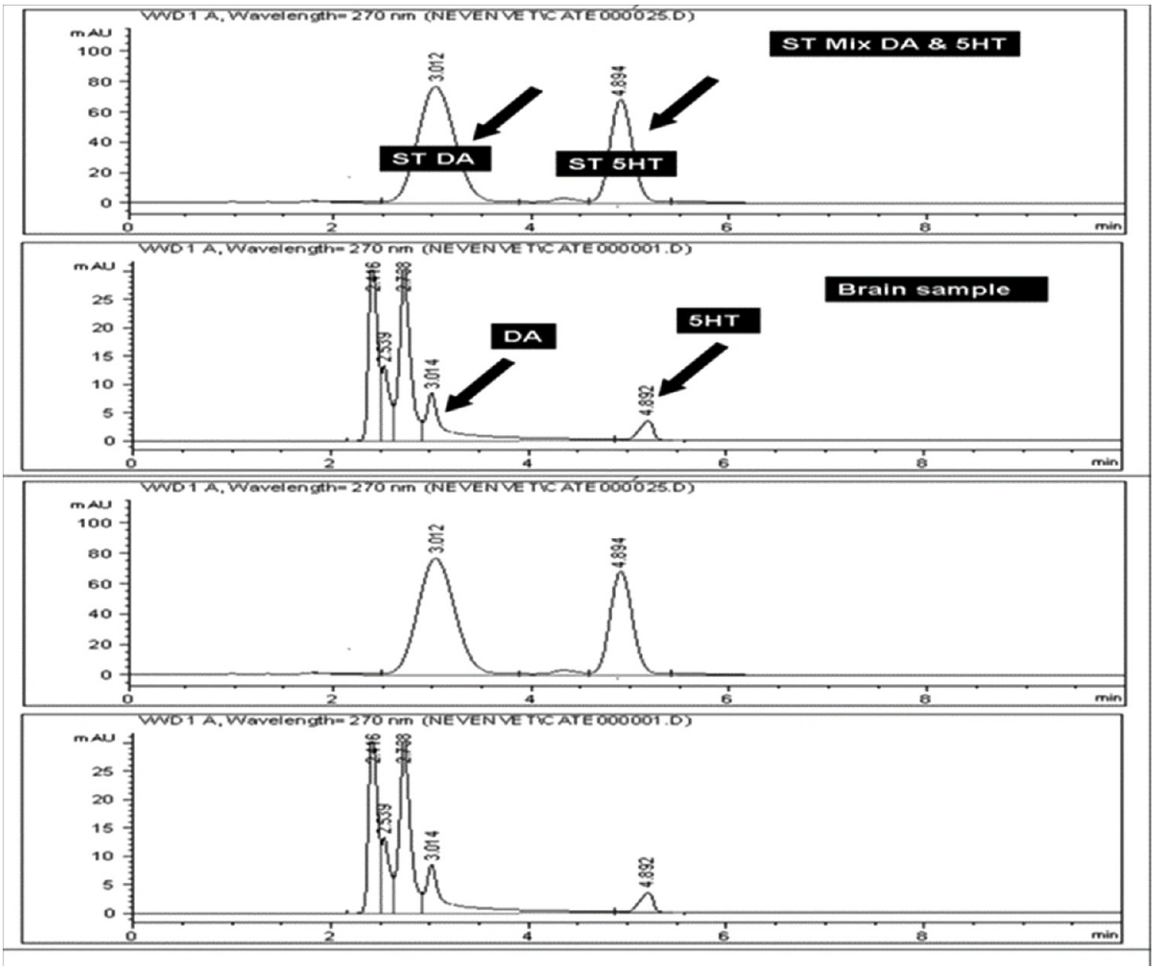

Figure 1. continued

https://doi.org/10.1021/acsomega.2c08295
ACS Omega 2023, 8, 18491−18508

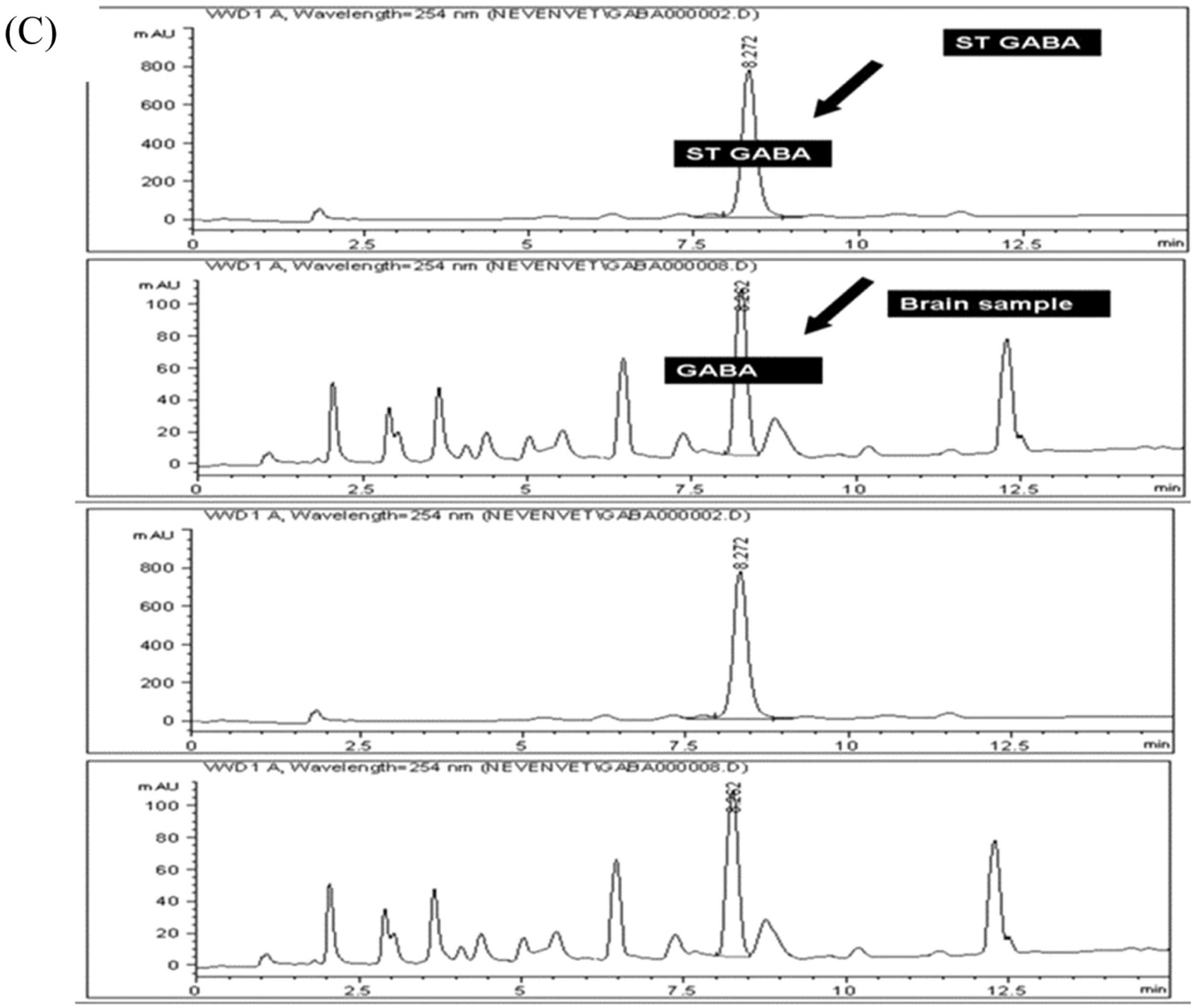

Figure 1. (A) Representative UPLC-MS base-peak chromatogram of the *O. majorana* aerial parts' methanol extract in negative ionization mode and some neurotransmitters (B) dopamine (DA), serotonin (5HT), and (C) GABA in the brain sample obtained from different treated groups.

melting curves were recorded in each reaction by regularly raising the temperature from 65 to 90 °C. The assay was generated using duplicates for each sample and included a no-template control to screen DNA contamination. The ACTB was used as an internal control to normalize the expression values with the $2^{-\Delta\Delta Ct}$ method.

2.10. Histopathological Examinations. Whole brain hemispheres were collected, fixed for 48 h in 10% neutral buffered formalin (pH 7.0), purified by alcohol and xylene, embedded in paraffin wax on the dorsolateral side, sliced at 4.5 μm to obtain sections to be stained with H&E, and examined under an Olympus light microscope (28).

The degree of intensity of the detected microscopic changes was evaluated using a multiparametric semiquantitative scoring system (classical technique) based on the percentage of tissue damage. The following scale: none (−), mild (+), moderate (++), severe (+++), and extensively severe (++++) was used and corresponded to 0, <12, 12−25, 25−50, and >50% tissue damage, respectively. In order to assess the following criteria, gliosis, neuronal degeneration, edema, and bleeding, seven microscopic fields/5 sections, which represented five rats per group, were blindly examined.[30]

2.11. Immunohistochemical Staining. The protein expression of inducible nitric oxide synthase (iNOS, a sensor for oxidative stress damage and neuroinflammation) as well as caspase-3 and bax (indicators for apoptosis) were localized by immunohistochemical labeling in paraffin-embedded brain tissue sections. Briefly, several primary antibodies were incubated on brain slices (Abcam Ltd.) before the secondary antibody and other reagents (Vectastain ABC-HRP Kit, Vector Laboratories) were applied. Each slide is peroxidase-labeled and DAB-chromogen substrate-colored (Sigma). According to the procedure outlined by Khalaf et al., the mean percentage area of various immunostaining positive reactions was calculated using Image J software.[31]

2.12. Statistical Analysis. Data are illustrated as the mean ± standard deviation of the mean (SD). The recorded results from various measurements were examined by one-way analysis of variance (ANOVA) and post hoc Duncan's test using the statistical package program (SPSS version 25); P values ≤ 0.05 represent statistical significance between groups.

https://doi.org/10.1021/acsomega.2c08295
ACS Omega 2023, 8, 18491−18508

Table 2. Peak Assignments of Metabolites in the 80% Methanol Extract of Aerial Parts of *Origanum marjoram* Using UPLC-MS in Negative Ionization Mode

peak no.	assignment	molecular formula	RT (min)	precursor ion m/z $[M-H]^-$	product ions MS/MS	chemical class	references
1	caffeic acid hexoside	$C_{15}H_{18}O_9$	0.67	341.1630	179, 161, 143, 119, 101	hydroxycinnamic acid	35
2	quinic acid	$C_7H_{12}O_6$	0.78	191.1080	171, 127, 111	organic acid	35, 36
3	arbutin	$C_{12}H_{16}O_7$	0.98	271.1387	108	hydroquinone	68, 69
4	syringic acid	$C_9H_{10}O_5$	1.19	197.1165	179, 135, 123, 73	hydroxybenzoic acid	36
5	dihydrocaffeic acid	$C_9H_{10}O_4$	2.34	181.0608	137, 109	hydroxyphenyl propanoic acid	37
6	syringic aldehyde	$C_9H_{10}O_4$	4.75	181.0816	153, 121	hydroxybenzaldehyde	38
7	unidentified	$C_{25}H_{28}O_4$	5.63	391.1824	281, 237, 221, 159, 137, 113, 109, 95, 71, 59		
8	caffeoyl-arbutin	$C_{21}H_{22}O_{10}$	5.82	433.1913	161, 109, 101	hydroxycinnamic acid	36
9	luteolin-glucuronide	$C_{21}H_{18}O_{12}$	6.04	461.1433	285, 179	flavone derivative	35, 39
10	rosmarinic acid hexoside	$C_{24}H_{26}O_{13}$	6.18	521.2296	359, 197, 179, 161, 71	hydroxycinnamic acid derivative	40 41
11	sagerinic acid	$C_{36}H_{32}O_{16}$	6.43	719.2682	359, 197, 179, 161, 135	cyclobutane lignan	41
12	apigenin-glucuronide	$C_{21}H_{18}O_{11}$	6.58	445.1649	269, 191, 149, 175, 113	flavone derivative	39, 41
13	rosmarinic acid	$C_{18}H_{16}O_8$	6.75	359.1291 719.2636 $(2M-H)^-$	197, 179, 161, 135	hydroxycinnamic acid	42, 43
14	lithospermic acid	$C_{27}H_{22}O_{12}$	7.05	537.1879	493, 359, 295, 197, 161	hydroxycinnamic acid	36, 39, 40
15	tri-*O*-methylellagic acid	$C_{17}H_{12}O_8$	7.31	343.1474	241, 221, 201, 169, 137, 123	ellagic acid derivative	44
16	salvianolic acid A	$C_{26}H_{22}O_{10}$	7.44	493.1915	295, 179, 161, 135,109	hydroxycinnamic acid	45
17	methyl salvianolate H/I	$C_{28}H_{24}O_{12}$	7.57	535.1453 551.2021	321, 319, 249, 231, 218, 195	hydroxycinnamic acid	43
18	luteolin	$C_{15}H_{10}O_6$	7.61	285.1063	229, 213, 151	flavone	36
19	carnosol	$C_{20}H_{26}O_4$	7.96	329.1142	272, 269, 209, 173	diterpenoid	46
20	apigenin	$C_{15}H_{10}O_5$	8.41	269.1236	225, 197, 159, 151, 117	flavone	36
21	rosmanol methyl ether	$C_{18}H_{16}O_8$	8.53	359.1480	283, 214, 197, 179, 95	hydroxycinnamic acid	47
22	trihydroxy octadecadienoic acid	$C_{18}H_{32}O_5$	8.74	327.2953	247, 211, 183, 171, 119, 85	fatty acid (oxylipid)	36
23	trihydroxy octadecenoic acid	$C_{18}H_{33}O_5$	9.30	329.3123	261, 247, 311, 293, 211, 197, 149, 113	fatty acid (oxylipid)	36
24	eriodictyol	$C_{15}H_{12}O_6$	9.62	287.2954	285, 135, 97	flavanone	43
25	dihydrokaempferide	$C_{15}H_{10}O_7$	9.72	301.1392	165, 161, 135, 121, 109	flavanonol	36
26	6-methylscutellarein	$C_{16}H_{12}O_6$	9.87	299.1133	284, 283, 266	flavone derivative	44
27	sakuranetin	$C_{16}H_{13}O_5$	10.96	285.1319	165, 145, 136, 119, 93, 65	flavanone derivative	36
28	hydroperoxy octadecadienoic acid	$C_{18}H_{32}O_4$	11.87	311.3329	223, 155, 127, 87	fatty acid (oxylipid)	36
29	hydroxylinolenic acid	$C_{18}H_{30}O_3$	14.16	293.2877	273, 183, 171, 121	fatty acid (oxylipid)	48
30	hederagenin	$C_{30}H_{48}O_4$	14.93	471.4283	405, 393	triterpenoid	44
31	hydroxyoctadecadienoic acid (hydroxylinoleic acid)	$C_{18}H_{32}O_3$	15.34	295.3028	277, 237, 223,137, 121, 43	fatty acid (oxylipid)	48
32	unidentified	$C_{34}H_{52}O_6$	15.60	555.3713	299, 225, 167, 135,		
33	unidentified	$C_{35}H_{62}O_6$	16.43	577.4508	281		
34	ursolic acid	$C_{30}H_{48}O_3$	19.11	455.4471	411, 251, 249, 248, 193, 162, 151	triterpenoid	44, 49
35	octadecatrienoic acid	$C_{18}H_{30}O_2$	19.20	277.2989	209, 185	fatty acid (oxylipid)	48
36	octadecadienoic acid	$C_{18}H_{32}O_2$	20.80	279.3151	279, 211, 126	fatty acid (oxylipid)	18, 48
37	hexadecanoic acid	$C_{16}H_{32}O_2$	22.40	255.3282	211, 191, 158, 152, 121, 59	fatty acid (oxylipid)	48

2.13. Molecular Docking. Computational studies were carried out using Discovery Studio 4.1 for docking studies of the tumor necrosis factor and MOE2010 software for docking studies of inducible nitric oxide synthase. The crystal structure of TNF-α with a small molecule inhibitor[32] was downloaded from PDB with code: **2AZ5**, while the murine inducible nitric oxide synthase oxygenase domain (Delta 114) 1-benzo[1,3]-dioxol-5-ylmethyl-3*S*-(4-imidazol-1-yl-phenoxy)-piperidine complex[33] was also downloaded from PDB with code: **2ORT**. The structures of the four selected phytochemicals: linalool, rosmarinic acid, γ-terpene, and terpene-4-ol were downloaded from PUBCHEM with the extension.sdf. The TNF-α protein was cleaned and corrected for missing amino acids. Hydrogens were added, and a simulation using CHARMm as the full charge and MMFF as the partial charge was applied. Heavy atoms were created, and protein atoms were set rigid via fixed atom constraints application. Minimization of proteins was confined using the adopted basis NR protocol. The output was then defined as a receptor, and the binding site was addressed via the inhibitor complex attached. The four selected compounds were then prepared as ligands together with the complexed inhibitor. The application of a similar forcefield to that of proteins was performed, except that the compounds to be docked are set flexible. The C-docker protocol was adopted, and the obtained 10 conformations of each compound were sorted according to their −(c-docker interaction energy). The two-dimensional (2D) and three-dimensional (3D) modes were viewed via Discovery Studio view tools. Regarding the nitric oxide synthase crystal structure downloaded from the PDB, we added hydrogen atoms, removed water molecules

https://doi.org/10.1021/acsomega.2c08295
ACS Omega 2023, 8, 18491−18508

Table 3. Effect of Imidacloprid (IMI) and/or the *O. majorana* Essential Oil (OMO) or Methanolic Extract (OME) on Some Neurobehavioral Parameters[a]

animal group test	control	OMO	OME	IMI	IMI + OMO	IMI + OME
			Open Field Test			
freezing	40.00 ± 7.50[a]	40.20 ± 7.58[a]	41.30 ± 7.50[a]	156.00 ± 9.27[b]	43.00 ± 7.68[a]	50.60 ± 7.07[a]
crossing no.	39.20 ± 3.06[a]	40.80 ± 3.17[a]	39.80 ± 2.48[a]	13.20 ± 5.26[b]	38.20 ± 3.5[a]	36.20 ± 2.76[a]
rearing	1.40 ± 0.24[a]	1.20 ± 0.20[a]	1.40 ± 0.25[a]	6.40 ± 0.74[b]	1.60 ± 0.40[a]	2.60 ± 0.68[a]
urination no.	0.40 ± 0.25[a]	0.60 ± 0.40[a]	1.00 ± 0.32[a]	2.80 ± 0.37[b]	0.60 ± 0.24[a]	1.20 ± 0.37[a]
defecation no.	1.00 ± 0.45[a]	1.40 ± 0.25[a]	1.20 ± 0.37[a]	4.80 ± 0.58[b]	1.00 ± 0.45[a]	1.80 ± 0.75[a]
			Forced Swim Test			
time spent swimming	218.20 ± 2.00[a]	220.00± 1.82[a]	219.00 ± 2.07[a]	86.00 ± 2.91[b]	207.20 ± 2.31[c]	202.60 ± 2.52[c]
time spent forced swimming	21.80 ± 2.00[a]	20.00 ± 1.82[a]	21.00 ± 2.07[a]	156.00 ± 4.30[b]	32.80 ± 2.31[c]	37.40 ± 2.52[c]
			Y-Maze Test			
% alteration behav.	89.00 ± 5.09[a]	91.80 ± 5.56[a]	90.60 ± 4.47[a]	5.60 ± 1.21[b]	82.00 ± 5.63[a]	83.60 ± 5.08[a]

[a]Data are expressed as the mean ± standard error of the mean (SEM) for 7 rats/group. *a*, *b*, *c* means having different superscript letters in the same row differ significantly at ($P \leq 0.05$).

using the software and then, energy minimization was carried out. After forcefield application, the receptor pocket and ligand (Heme + complex inhibitor) was defined and selected for docking. The enzyme was also set fixed and the downloaded four compounds from PUBCHEM were opened as.moe files, energy minimized, and set flexible for docking. The docking protocol was performed using an α triangle, and 30 conformations were produced for each ligand. The conformations were sorted according to the energy scores applied and the 2D view was generated using MOE.

3. RESULTS

3.1. Gas Chromatography−Mass Spectrometry (GC−MS) Metabolite Identification in *O. majorana* Essential Oil (OMO). The volatile constituents in the essential oil of *O. majorana* grown in Egypt were detected with relative ratios as recorded corresponding to their order of elution on Rtx-5MS fused bonded columns in a previous study.[34] This led to the identification of a total of 55 components. The most abundant volatile metabolites representative of OME were linalool (17.76%), γ-terpinen (14.26%), terpinen-4-ol (13.54%), α-terpinene (8.21%), *cis*-sabinene hydrate (5.89%), sabinene (5.62%), α-terpineol (4.74%), linalyl acetate (3.64%), terpinolene (3.32%), and limonene (3.25%) all belonging to the oxygenated and hydrocarbon monoterpenoid group.

3.2. UPLC-MS Qualitative Profiling of the *O. majorana* Methanol Extract. The base-peak chromatogram of the methanol extract of *O. majorana* aerial parts is displayed in Figure 1. Reversed-phase UPLC-MS analysis and associated data previously stated in the literature led to the identification of 37 constituents in the examined methanol extract summarized in Table 2, according to their elution order indicated with the numbers 1−37. The identified metabolites were classified into four groups, including 10 phenolic acids, 8 flavonoids, 8 fatty acids, and 8 metabolites belonging to other groups, and 3 unidentified metabolites. The extract was analyzed in negative electrospray ion (ESI) mode, and the compounds are documented with their retention times, molecular formulae, $[M - H]^-$, MS, and MS^2 data, and the suggested identification and chemical classes of the compounds. All of the found components in this work were tentatively identified by their MS and MS^2 data, compared to that reported in the literature.

3.2.1. Phenolic Metabolites. Ten phenolic acids belonging to hydroxycinnamic, hydroxybenzoic, and hydroxyphenyl propanoic acid subclasses were identified in the *O.majorana* methanol extract. Hydroxycinnamic acid derivatives were identified as follows: rosmarinic acid (peak **13**) with molecular masses of 359.1291 $(M - H)^-$ and 719.2636 $(2M - H)^-$ and the MS^2 provided fragments at *m/z* 197, 179, 161, and 135 rosmarinic acid hexoside (peak **10**) revealed a fragmentation pattern by loss of 162 Da (glycosidic moiety), and this gave rise to the aglycone rosmarinic acid (*m/z* 359). Lithospermic acid peak **14** presented an ion at $(M - H)^-$ *m/z* 537; it was confirmed by its fragments at *m/z* 493, 359, 295, 197, and 161. Caffeic acid hexoside (peak **1**) with $(M - H)^-$ 341.1630 and a base peak of 179, caffeoyl-arbutin **8** ($(M - H)^-$ *m/z* 433), as well as salvianolic acid A **16** ($(M - H)^-$ *m/z* 493), methyl salvianolate H/I **17** ($(M - H)^-$ *m/z* 535), and rosmanol methyl ether **21** (*m/z* 359) were identified. Syringic acid **4** was the only detected hydroxybenzoic acid at *m/z* 197, showing ms/ms fragments at 179, 135, 123, and 73. Dihydrocaffeic acid **5**, a hydroxyphenyl propanoic acid, showed the $(M - H)^-$ ion at *m/z* 181.0608 and the MS^2 fragment at 137.

3.2.2. Flavonoids. Eight flavonoids were identified in the *O. majorana* methanol extract belonging to flavones, flavanones, and flavanonols. Flavone derivatives: luteolin-glucuronide (peak **9**, *m/z* 461) was identified by a fragmentation pattern that gave a fragment ion at *m/z* 285 (luteolin) by loss of 176 Da (glucuronic acid). Peak **12** was identified as apigenin-glucuronide by MS data (*m/z* 445) and the fragmentation pattern that gave a fragment ion at *m/z* 269 (apigenin) by losing the glucuronic acid moiety [M-H-176]. Peak **18** was identified as luteolin (*m/z* 285) and **20** as apigenin (*m/z* 269). Peak **26**, with the $(M - H)^-$ ion *m/z* 299.1133, was characterized as 6-methylscutellarein by the MS and MS/MS data. The fragment ion at *m/z* 284 was due to the loss of CH_3 (15 Da), whereas the fragment ion at *m/z* 266 was the result of further loss of H_2O (18 Da). Flavanone derivatives: Peak **24** was identified as eriodictyol (*m/z* 287), and **26** was identified as sakuranetin (*m/z* 285). Flavanonol: Peak **25** (*m/z* 301) was characterized as dihydrokaempferide based on fragments at *m/z* 165 ($^{0,1}A^-$ ring fragmentation) and 135 ($^{1,2}A^-$ ring fragmentation).

3.2.3. Fatty Acids. Eight fatty acids were detected in *O. majorana* aerial parts' methanol extract. Several unsaturated hydroxy fatty acids: trihydroxy octadecadienoic **22**, trihydroxy octadecenoic **23**, hydroperoxy octadecadienoic **28**, hydroxylinolenic **29**, and hydroxyoctadecadienoic (hydroxylinoleic) **31** acids were identified by loss of a water molecule. In

https://doi.org/10.1021/acsomega.2c08295
ACS Omega 2023, 8, 18491−18508

Table 4. Effect of Imidacloprid (IMI) and/or the *O. majorana* Essential Oil (OMO) or Methanolic Extract (OME) on AchE and Some Neurotransmitter Levels[a]

animal group levels	control	OMO	OME	IMI	IMI + OMO	IMI + OME
AchE (moles/L/min × 10^6/g tissue)	1.49 ± 0.03[a]	1.48 ± 0.04[a]	1.47 ± 0.07[a]	0.73 ± 0.04[b]	1.26 ± 0.04[c]	1.25 ± 0.07[c]
DA (μg/g tissue)	1.38 ± 0.08[a]	1.42 ± 0.05[a]	1.23 ± 0.07[a]	0.58 ± 0.02[b]	0.94 ± 0.07[c]	0.92 ± 0.05[c]
5HT (μg/g tissue)	0.83 ± 0.02[a]	0.86 ± 0.02[a]	0.85 ± 0.02[a]	0.45 ± 0.01[b]	0.68 ± 0.02[c]	0.65 ± 0.02[c]
GABA (μg/g tissue)	4.61 ± 0.13[a]	4.29 ± 0.10[a]	4.38 ± 0.06[a]	2.54 ± 0.12[b]	3.85 ± 0.10[c]	3.75 ± 0.10[c]

[a]Data are expressed as the mean ± SEM for 7 rats/group. *a*, *b*, *c* means having different superscript letters in the same row differ significantly at ($P \leq 0.05$). AchE, acetylcholine esterase; DA, dopamine; 5HT, serotonin; and GABA, γ-aminobutyric acid.

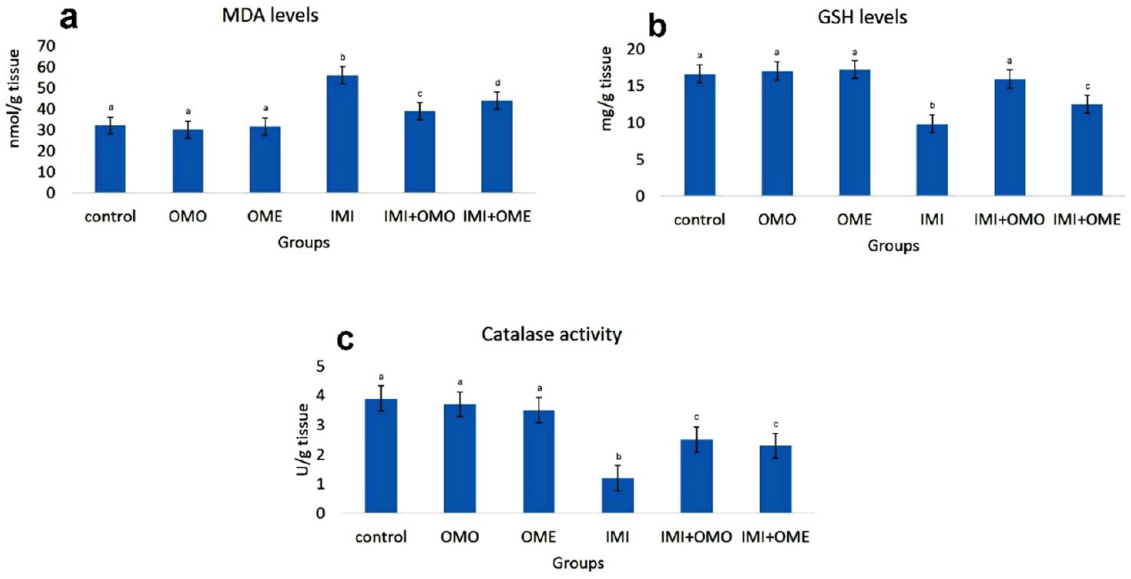

Figure 2. Effect of IMI and/or *the O. majorana* extract on some oxidative stress markers. (a) MDA levels, (b) GSH content, and (c) CAT activity in the brain homogenates of different groups. Data are expressed as the mean ± SEM for 7 rats/group. *a*, *b*, *c* means having different superscript letters in the same row differ significantly at ($P \leq 0.05$). IMI, imidacloprid; OMO, *O. majorana* essential oil; and OME, *O. majorana* methanol extract.

addition to two unsaturated fatty acids, octadecatrienoic **35** and octadecadienoic (linoleic) **36** acids and one saturated fatty acid was identified as hexadecanoic acid (palmitic acid) (peak **37**). All were tentatively identified from their mass spectra, as displayed in Table 2.

3.2.4. Others. Other detected metabolites were an organic acid (peak **2**) identified as quinic acid with $[M - H]^-$ at m/z 191, arbutin, hydroquinone (peak **3**) with $[M - H]^-$ at m/z 271, syringic aldehyde, a hydroxybenzaldehyde m/z 181.0816 (peak **6**), a cyclobutane lignan (peak **11**) annotated as sagerinic acid (m/z 719.2682), and tri-*O*-methylellagic acid **15** m/z 343, an ellagic acid derivative. In addition to a diterpenoid **19** identified as carnosol (m/z 329.1142) and two triterpenoids, hederagenin (peak **30**) $[M - H]^-$ at m/z 471.4283 and ursolic acid **34** at m/z 455.4471 were identified.

3.3. Behavioral Assay. *3.3.1. Open Field.* IMI exposure resulted in an anxiogenic profile of behavioral changes, as evidenced by more time spent freezing, number of rearing, as well as higher urination and defecation scores with lower levels of horizontal locomotion. However, coadministration of IMI with either the oregano oil or methanol extract significantly decreased levels of IMI-induced anxiety-like behavior since no significant difference was found in any of the recorded parameters compared to their control group (Table 3).

3.3.2. Forced Swim Test. Exposure to IMI caused a significant elevation in the immobility period. However, concurrent administration of IMI with either origanum oil or the extract form could reduce the immobility period compared to the IMI-received group. Moreover, the administration of oregano oil form significantly alleviated IMI-induced depressive-like behavior than methanolic extract form, where rats in the oil-ameliorated group had an antidepressant effect as their control littermates (Table 3).

3.3.3. Spatial Y-Maze Memory Test. Exposure to IMI caused a significant impairment of the short-term spatial memory in the Y-maze, as indicated by reducing the spontaneous alternation behavior percentages in comparison with rats in all other treatments. However, rats coadministered with either oregano oil or extract form significantly enhanced spatial cognition ability compared to the IMI-received group. Furthermore, the administration of oregano oil remarkably mitigated IMI-induced spatial memory impairment than methanolic extract form, with rats in the oil-ameliorated group performing as well as their controls in the Y-maze test (Table 3).

3.4. AchE Activity and Neurotransmitter Concentrations. The activity of AchE was significantly reduced after exposure to IMI when compared to the control group, while origanum administration, either the methanol or oil extract showed significant amelioration if compared with the IMI group. On the other hand, both treated groups showed a substantial reduction if compared to the control group. Concerning DA, 5HT, and GABA levels, there was a considerable reduction in the abovementioned neurotransmitters in the brain of rats receiving IMI in comparison with the control group. *O. majorana* administration, either methanol or

https://doi.org/10.1021/acsomega.2c08295
ACS Omega 2023, 8, 18491−18508

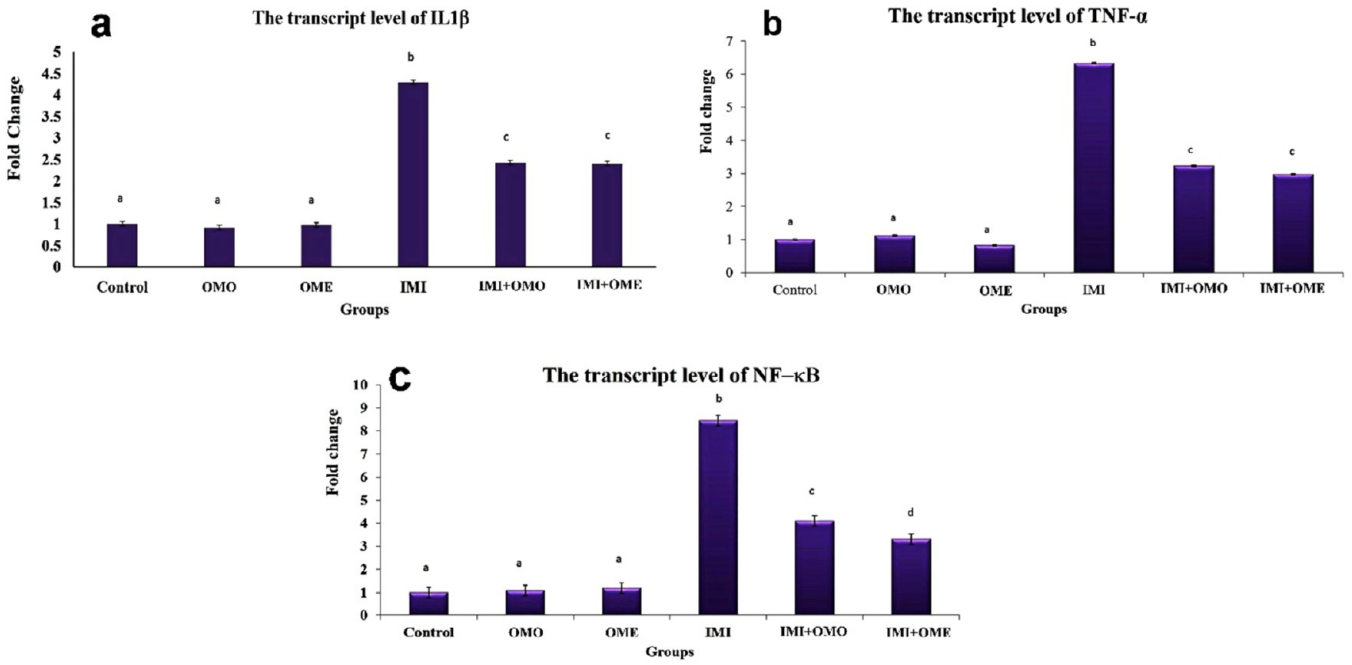

Figure 3. Effect of IMI and/or the *O. majorana* extract on the transcriptase levels of the studied genes. (a) IL-1*β*, (b) TNF-*α*, (c) NF-*κ*B in the brain homogenates of different groups. Data are expressed as the mean ± SEM for 7 rats/group. *a*, *b*, *c* means having different superscript letters in the same row differ significantly at ($P \leq 0.05$). IMI, imidacloprid; OMO, *O. majorana* essential oil; and OME, *O. majorana* methanol extract.

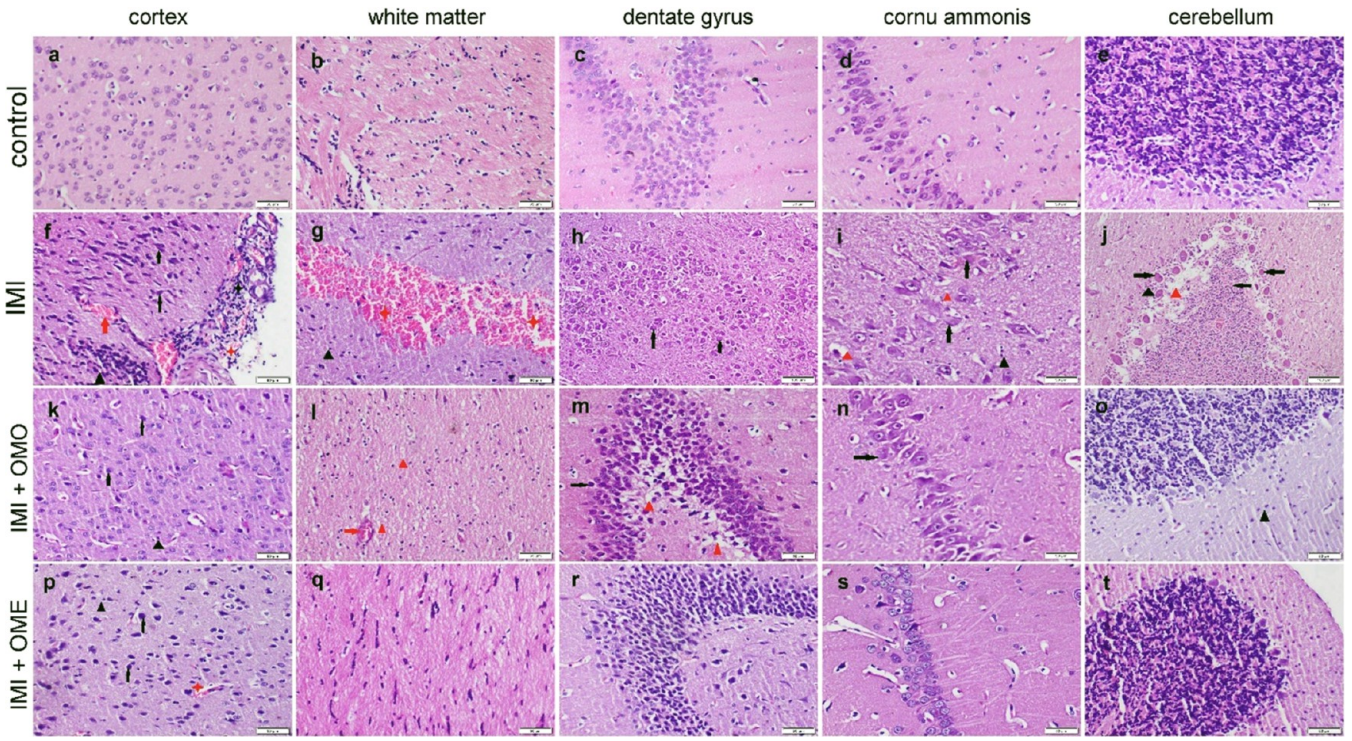

Figure 4. Photomicrograph of brain tissue sections at different areas which stained with hematoxylin and eosin (H&E) and represented different treatment groups. (a−e) Control group showed normal histological structure in different brain areas. (f−j) IMI receiving group showed neuronal degeneration and necrosis (black arrows), gliosis (black triangles), inflammatory cells infiltration (black stars), congestion (red arrows), vacuolation (red triangles), and extravasation of RBCs (red stars) in different brain areas. (k−o) IMI + OMO receiving group showed mild neuronal degeneration (black arrows), gliosis (black triangles), congestion (red arrows), and vacuolation (red triangles), in some brain areas. (p−t) IMI + OME receiving group showed moderate neuronal degeneration (black arrows), minimum gliosis (black triangle), and RBCs extravasation (red star) in the neocortex while other brain areas showed normal histological structure. IMI, imidacloprid; OMO, *O. majorana* essential oil; and OME, *O. majorana* methanol extract.

oil extract, revealed a significant elevation in these levels when compared with the IMI group. However, the best results were observed in the *O. majorana* oil-treated group (Table 4 and Figure 1).

https://doi.org/10.1021/acsomega.2c08295
ACS Omega 2023, 8, 18491−18508

Table 5. Microscopic Lesion Scoring in Different Brain Areas of Treated Rats[a]

	control	OMO	OME	IMI	IMI + OMO	IMI + OME
Histological Grading of the Forebrain Lesions (Cerebrum)						
neuronal degeneration	−	−	−	++++	+	++
gliosis	−	−	−	++++	+	++
edema	−	−	−	+++	−	++
hemorrhage	−	−	−	+++	−	−
Histological Grading of the Midbrain Lesions (Striatum and Hippocampus)						
neuronal degeneration	−	−	−	++	+	−
gliosis	−	−	−	+	+	−
edema	−	−	−	+	+	−
hemorrhage	−	−	−	−	−	−
Histological Grading of the Hindbrain Lesion (Cerebellum)						
neuronal degeneration	−	−	−	++	+	+
gliosis	−	−	−	++	−	−
edema	−	−	−	+++	−	+
hemorrhage	−	−	−	+	−	−

[a]Histological lesion scoring was assessed as follows: (−) normal histology, (+) mild, (++) moderate, (+++) severe, and (++++) extensive severe tissue damage. n = 7 rats/group. IMI, imidacloprid; OMO, *O. majorana* essential oil; and OME, *O. majorana* methanol extract.

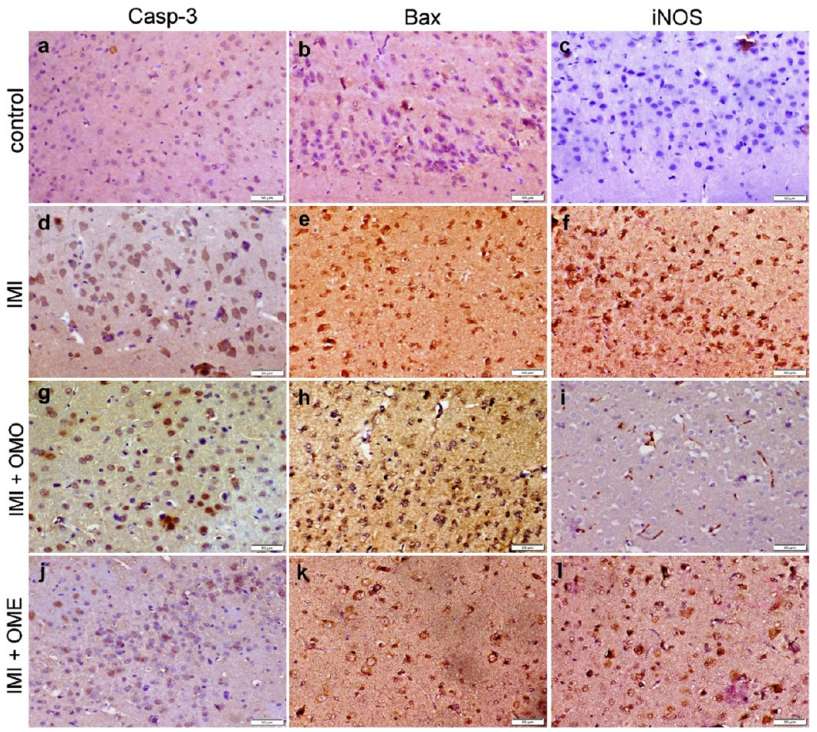

Figure 5. Photomicrograph representing Casp-3, Bax, and iNOS immunostaining of the cerebral cortex in different treatment groups. (a−c) Control group showed negative expression of the above immune markers. (d−f) IMI receiving group showed strong positive immunoexpression of the studied protein markers. (g−i) IMI + OMO receiving group showed mild to moderate Casp-3 and Bax immunoexpression with negative iNOS expression. (j−l) IMI + OME receiving group showed moderate positive immunoexpression of the studied protein markers. IMI, imidacloprid; OMO, *O. majorana* essential oil; and OME, *O. majorana* methanol extract.

3.5. Oxidative Stress Evaluations. A significant elevation in MDA levels was associated with a significant reduction in the GSH and CAT activity in the group receiving IMI compared to the control group. On the other hand, cotreatment with origanum either oil or methanolic extract with IMI could markedly decrease MDA levels and increase the GSH and CAT activity compared to the IMI group, but the best results were observed in the oregano oil-treated group (Figure 2).

3.6. Quantitative RT-PCR Analysis for IL-1β, TNF-α, and NF-κB Genes. The IMI administration resulted in a significant upregulation of NF-κB, IL-1, and TNF-α mRNA levels. This upregulation is markedly ameliorated in the *O. majorana* oil and methanol extract-treated groups. Both the oil and methanol extract provided potent protection against the IMI. There was an insignificant difference between them except for the NF-κB, such that the extract showed a significant protective effect compared to the oil (Figure 3).

3.7. Histopathological Examinations. Brain tissue sections obtained from the control group and those receiving both *O. majorana* oil and the methanol extract showed regular histological organization in different brain areas, including the

https://doi.org/10.1021/acsomega.2c08295
ACS Omega 2023, 8, 18491−18508

Table 6. Interaction Energy/Score Results of Phytochemicals and Reference Inhibitors against TNF-α and iNOS

compound	-(c-docker interaction energy) (kcal/mol) against 2AZ5 (TNF-α)	binding mode	-(energy score) (kcal/mol) against iNOS 2ORT	binding mode
reference inhibitor (6,7-dimethyl-3-[(methyl{2-[methyl({1-[3-(trifluoromethyl)phenyl]-1*H*-indol -3-yl}methyl)amino] ethyl}amino)methyl]-4H-chromen-4-one)	−39.25	H-bond: B:Tyr 59, B:Gly 121, B: Gly 122 (x2) Pi−Pi bond: A:Leu 57, B: Tyr 59 (x2), B: Tyr 119, B:Leu 120, B: Tyr 151		no heme complexation.
reference			−8.82	polar exposure to Cys 194 and Arene-H to Phe 363
linalool	−21.71	Pi−Pi bond: A:Tyr 59, B:Tyr 59, B:Tyr 119, B: Tyr 151	−9.41	ligand exposure to heme. Polar exposure to Cys 194 and Arene-H to Cys 194 and Phe 363
rosmarinic acid	−39.25	H-bond: B:Leu 120, A:Gly 121	−12.96	metal complex with heme.
		Pi−Pi bond: A:Tyr 119, B:Tyr 119		polar exposure and Arene-H to Cys 194
γ-terpene	−20.72	Pi−Pi bond: A:Tyr 59, B:Tyr 119, B:Tyr 151	−8.07	showed no interaction
terpene-4-ol	−24.23	H-bond: B:Ser 60, B:Leu 120	−8.94	metal complex to heme.
		Pi−Pi bond: B:Leu 52, B:Tyr 119 (x2), B:Tyr 151		

https://doi.org/10.1021/acsomega.2c08295
ACS Omega 2023, 8, 18491−18508

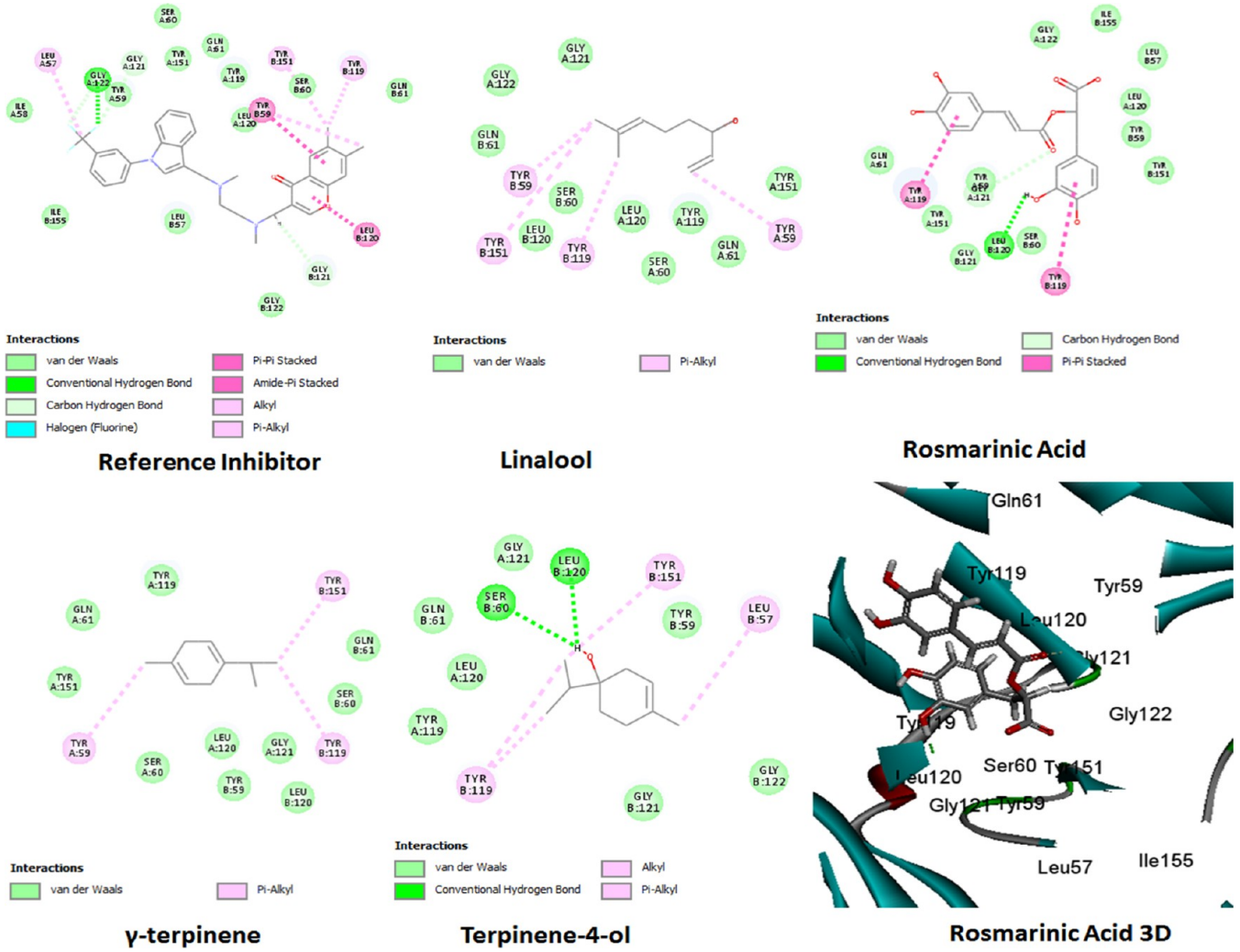

Figure 6. 2D interaction diagrams of linalool, rosmarinic acid, γ-terpene, terpene-4-ol, and the reference inhibitor against TNF-α, and the 3D interaction diagram of the most active rosmarinic acid (Discovery Studio software).

cerebrum cortex, white matter, hippocampus, and cerebellum (Figure 4a–e). Otherwise, the IMI receiving group showed a wide range of pathological alterations in different brain areas. Meninges showed congestion, hemorrhage, and diffuse inflammatory cell infiltration. Most neurons in the cerebral cortex showed degeneration and necrosis accompanied by neuronophagia and extensive gliosis (Figure 4f). The white matter showed focal to diffuse gliosis and severe hemorrhage (Figure 4g). The hippocampus showed disorganization and widespread neuronal necrosis in different parts, especially DG, CA2, and CA3 zones (Figure 4h,i). The cerebellum showed vacuolation along with extensive neuronal necrosis and gliosis in both the Purkinji and granular cell layers (Figure 4j). Cotreatment of either the *O. majorana* oil or methanol extract with IMI could improve the microscopic pictures of different brain areas. Regarding the oil-treated group, the cerebral cortex and white matter showed mild neuronal degeneration and gliosis (Figure 4k,l). The hippocampus displayed sporadic cell necrosis and mild vacuolation in the DG, along with a normal microscopic picture of the CA3 zone (Figure 4m,n). Additionally, the cerebellum showed normal histological organization (Figure 4o). Likewise, the methanolic extract-treated group nearly showed similar results to the oil-treated group but differed in its degree of severity. Moderate neuronal degeneration and gliosis were observed in the cerebral cortex along with a normal microscopic picture of other brain areas (Figure 4p–t).

Table 5 shows a summary of the histopathological alteration scoring that demonstrates the highest score in all parameters in the IMI group. Otherwise, cotreatment of origanum, either oil or methanolic extract with IMI, markedly reduced this score; however, the best improvement was observed in the oil-treated group.

3.8. Immunohistochemical Staining. The repeated oral intake of IMI resulted in marked neuronal apoptosis manifested by strong Casp-3 and Bax immunostaining expression. Additionally, the strong immunopositivity of iNOS was also recorded in the IMI receiving group. In contrast to the IMI group, groups that were cotreated by either *O. majorana* oil or the methanol extract along with IMI exhibit weak positive to negative immunostaining responses of all of the abovementioned immune markers in different brain regions, mainly the cerebral cortex (Figure 5).

3.9. Molecular Docking Study. The promising compounds out of the addressed phytochemicals were selected as linalool, rosmarinic acid, γ-terpene, and terpene-4-ol and utilized to investigate their possible mechanism of actions via *in silico* molecular modeling studies. Two targets were selected

https://doi.org/10.1021/acsomega.2c08295
ACS Omega 2023, 8, 18491−18508

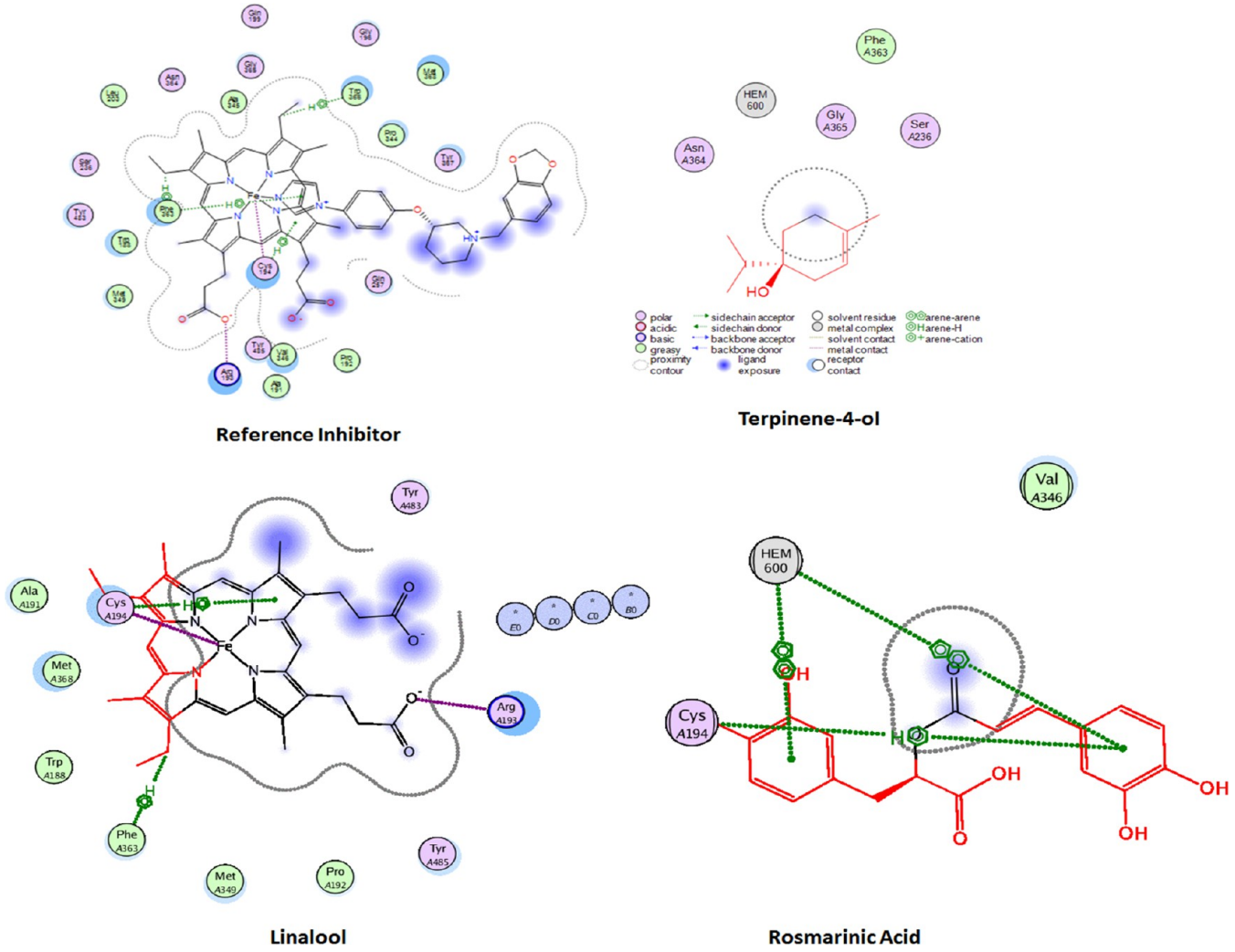

Figure 7. 2D interaction diagrams of linalool, rosmarinic acid, terpene-4-ol, and the reference inhibitor against iNOS (MOE2010).

for the study: TNF-α[32] and iNOS.[33] Both were downloaded from PDB under codes: **2AZ5** and **2ORT**, respectively. The molecular docking study was first applied between the four compounds and TNF-α via Discovery Studio 4.1 utilizing the C-docker protocol. The results were compared to that of the reference ligand—small molecule inhibitor—already complexed with the protein and downloaded from PDB: 6,7-dimethyl-3-[(methyl{2-[methyl({1-[3-(trifluoromethyl)-phenyl]-1*H*-indol-3-yl}methyl) amino]ethyl} amino)methyl]-4*H*-chromen-4-one. The reference showed (c-docker interaction energy) = −39.25 kcal/mol while the compounds were in the range of −(39.25−20.72) kcal/mol, as shown in Table 6. The four compounds were competitive to the reference at the active site, as shown in Figure 6, with the priority to the most active rosmarinic acid that showed equivalent interaction energy and binding to key amino acids Tyr 119 and Leu 120. On the other hand, the molecular docking study was applied against iNOS using MOE2010 since it contains the heme structure with iron metal, and Discovery Studio does not read metal interactions. The complexed inhibitor reference: (3*S*)-1-(1,3-benzodioxol-5-ylmethyl)-3-[4-(1*H*-imidazol-1-YL)-phenoxy]piperidine, showed an interaction score = −8.82 kcal/mol while the four compounds were in the range of −(12.96−8.07) kcal/mo,l as shown in Table 6. As shown in Figure 7, these compounds provided the metal complex/exposure to heme which strengthens the attachment in the pocket active site for inhibition compared to a reference, except for γ-terpene, which showed no interaction. Rosmarinic acid scored the best compared to the reference, and the arene H-bond to the key amino acid Cys 194.

4. DISCUSSION

Behavior results from what happens in the neurological system in both humans and animals; hence behavioral analysis is crucial for evaluating neural function.[50] The current study used motor activity monitoring as an example of motivated behavior, the most popular indicator of CNS dysfunction.[51] Three behavioral assays, the open field test, the forced swim test, and the Y-maze test, were carried out to evaluate the neurobehavior of rats after exposure to IMI and/or oregano, either oil or methanolic extract. The open field is a commonly used test for assessing emotionality-related conflict between a rat's exploratory tendency to wander into the center of the arena and safety by remaining in a corner or along the periphery.[52] Herein, rats exposed to IMI displayed a significant increase in their anxiety level and emotionality, visualized by increased immobility and decreased horizontal locomotion. Conversely to horizontal activity, higher levels of vertical locomotion of IMI-treated rats were observed in the open field's corners and against the wall upon first exposure, and this

https://doi.org/10.1021/acsomega.2c08295
ACS Omega 2023, 8, 18491−18508

could be attributed to novelty-induced more fear-related behavior and also rats' proclivity to escape.[53] Furthermore, elevated urination and defecation scores noticed in IMI-intoxicated animals are also effective and sensitive indicators of emotionality and anxiety.[54,55] The forced swim test has been widely used to assess behavioral despair because immobility demonstrates the level of depression.[56] In our study, IMI-administered rats showed decreased mobility time and increased immobility duration, reflecting the depressive condition in response to elevated stress levels.[57] The Y-maze assay is a behavioral test that depends on rats' motivation to explore novel habitats. Instead of returning to a previously explored arm of the maze, rats investigate a new one.[58,59] This behavior is influenced by several brain regions, including the prefrontal cortex, hippocampus, and basal forebrain.[60] Our findings revealed that rats treated with IMI had poor working spatial memory, judging by a decline in the spontaneous alternation percentage, a measure of rats' natural propensity to alternate among three different arms. These findings are in accordance with those reported by Kara and colleagues,[61] asserting that IMI caused learning and memory impairment in rats.

In the current study, the levels of neurotransmitters, including serotonin (5HT), γ-aminobutyric acid (GABA), and dopamine (DA) were significantly reduced in IMI-exposed rats. Neurotransmitters are among the neuronal molecules likely to be affected by stress leading to neurobehavioral disturbance. Depletion of neurotransmitters DA, GABA, and 5HT due to IMI administration was found to be in accordance with the results documented by Abd-Elhakim et al.[62] As the brain has a weak antioxidant defense mechanism and is very labile to oxidative stress threats due to its high lipid content and high energy demand when it exceeds its capacity to overcome free radicals and reactive oxygen species (ROS).[63] Thus, it can eventually lead to significant neuronal impairment.[64] ROS and free radicals participate significantly in the toxicity of pesticides and environmental chemicals, inducing oxidative stress and alterations in antioxidants or free radical scavenging enzymatic pathways.[65] The current study revealed a significant alteration in the brain redox status of the group exposed to IMI associated with a significant elevation of brain MDA level and a significant reduction in GSH and CAT activity in the rat brain. The same dysregulated brain redox status results associated with IMI were reported by Rawi et al.[63] Moreover, the oxidative damage of IMI was reported to be caused by increasing the protein oxidation and lipid peroxidation of the brain cells. In the case of oxidative stress, highly reactive molecules such as superoxide, peroxynitrite, and hydroxyl radical can accumulate in the body and cause permanent damage, mitochondrial dysfunction, synaptic transmission failure, and ultimately cell death.[66] Therefore, GABA reduction in the brain tissue of IMI-exposed rats could be attributed to oxidative stress, as neural oxidative damage can decrease the synthesis of GABA due to the imbalance in the neuronal redox potential. Oxidative insults are suggested to be associated with carbonyl modification of glutamine synthase and significant inhibition in its activity.[67] Similarly to the synthesis of GABA, as oxidative stress gets enhanced, DA synthesis is also inhibited, which is mediated by the reduction of tyrosine hydroxylase, the synthesizing enzyme, and the rate-limiting step of DA production through the formation of 3-nitrotyrosine by peroxynitrite, which may downregulate the activity of tyrosine hydroxylase.[66] Also, 5-HT levels were decreased in the IMI group, which could be attributed to the destruction of brain regions with a high density of serotonergic neurons due to oxidative damage induced by IMI administration.[68] Interestingly, our study shows a significant reduction in AchE activity due to IMI exposure. Our results were found to be in accordance with Bhardwaj et al.,[69] and Vohra et al.[70] Brain AchE inhibition suggested that several regions in the brain are subjected to significant damage.

All the previously mentioned findings were reconfirmed by the histological examination demonstrating widespread neuronal degeneration and neuronophagia accompanied by severe congestions and extensive gliosis in most brain areas. The observed lesions in the cerebral cortex, hippocampus, and cerebellum may explain the imbalance, loss of memory, and abnormal gait in rats, respectively. We suggest that these alterations are attributed to oxidative stress. Imidacloprid, like other pesticides, accelerated ROS generation in the brain tissue via glial cell stimulation and promoted oxido-inflammatory response and apoptosis via mitochondrial dysfunction.[71] Opening the mitochondrial transition pores and increasing the cytosolic calcium levels lead to cytochrome-c release that promotes the apoptosis mechanism.[72,73] Both ROS and cytochrome-c activate the proapoptotic proteins as Bax and Casp-3, as well as they can downregulate the anti-apoptotic proteins as Bcl2.[71] Neuroinflammation is another mechanism of IMI-induced neural toxicity and is also attributed to oxidative stress. ROS overgeneration could induce neuronal damage via peroxidation of membrane phospholipids and degradation of cytoskeletal proteins. These can attract a huge number of microglia cells to engulf the necrotic neurons. Microglia cells release and activate proinflammatory cytokines such as IL-1 and TNF-α and initiate the inflammatory response via modulating the NF-κB signaling pathway.[74]

This study showed that administration of *O. majorana* either in oil or extract form improved the cognitive abilities of IMI-exposed rats through significantly ameliorating effects in the brain AchE activity, DA, 5-HT, and GABA levels if compared with the imidacloprid group. Those changes could be correlated to the *O. majorana* antioxidant power. Moreover, *O. majorana* essential oil reverses neuroinflammation, apoptosis, and oxidative damage in rats.[75] The antioxidant properties of *O. majorana* have been previously confirmed.[76] It has been documented that antioxidants can block the reuptake of 5-HT, thereby increasing its availability in synaptic clefts.[77] The favorable impact of OMO improved the emotional condition of the IMI-treated rats by alleviating most of the adverse impacts caused by IMI due to its anxiolytic effect.[78] This result was proposed through the elevation of monoamine compounds in humans.[77] By studying the *Origanum* genus, Mombeini et al.[79] suggested that *oregano* extract averts the monoamine neurotransmitter degradation and increases extracellular 5-HT levels in the brain in a dose-dependent manner in anxiolytic mice. Recently, a group of researchers revealed that *O. majorana* essential oil exerted antidepressant-like effects by modulating serotonergic, dopaminergic, and noradrenergic systems.[77] Our findings agree with those of Amiresmaeili and his colleagues, who reported the antidepressant properties of oregano.[80]

Moreover, Postu et al. suggested that *O. majorana* essential oil promotes cognitive functions, reduces brain oxidative stress, and enhances memory function in Aβ1−42-treated rats.[81] This finding could explain our results about reducing MDA levels and increasing the GSH and CAT activity in the brain of rats

https://doi.org/10.1021/acsomega.2c08295
ACS Omega 2023, 8, 18491−18508

cotreated with either oregano oil or extract. Mossa and Nawwar postulated that the antiacetylcholinesterase activity might be due to the presence of terpenoids in oils which may act synergistically with other constituents.[82] Tunisian *O. majorana* essential oil displayed anti-ACHE activity that was assumed to be attributed to its high hydrocarbon or oxygenated monoterpene content.[83] Moreover, the chemical composition, along with the anti-neurodegenerative, antibacterial, and antioxidant activity of ethanol and aqueous extracts of *O. majorana* originating from four different places, i.e., Egypt, Greece, Libya, and Serbia, were investigated. The Egyptian sample ethanol extract recorded the highest phenolic and flavonoid contents. A high rosmarinic acid content, with the highest quantity in the Egyptian plant ethanol extract, was recorded using HPLC analysis. According to the previous results, sweet marjoram from Egypt could be recommended as a result of having the best antioxidant, antibacterial, acetylcholinesterase, and tyrosinase inhibitory activity.[84] Anticonvulsant and sedative activities for different extracts of aerial parts of *O. majorana* were investigated it was assumed that the occurrence of flavonoids, steroids, triterpenoids, and essential oil might be responsible for these activities.[85]

Molecular docking was projected to investigate the probable ligand-target interactions that might justify the perceived neuroprotective effects of the essential oil (OMO) and methanol extract (OME) against IMI-induced neurotoxicity in rats. Previous studies revealed that iNOS and nitric oxide are associated with neuroinflammatory reactions. Upregulation of iNOS generates large amounts of proinflammatory cytokines (Tumor necrosis factor-α, Interferon-γ, and Interleukin-1). TNF-α employs pathophysiological and homeostatic functions in the nervous system. TNF-α is a crucial part of neuroinflammatory reactions correlated with neurological disorders.[86] Our findings of the molecular docking study align very well with a previous report that stated the ability of rosmarinic acid to remarkably reduce the levels of inflammatory markers (TNF-α and iNOS) in chronic constriction injury rats. The neuroprotective actions of rosmarinic acid are attributed to its antioxidant and anti-inflammatory activities.[87] Similarly, linalool has been reported to alleviate TNF-α and iNOS in mice with a liver injury induced using lipopolysaccharide/d-galactosamine. This effect is due to the ability of linalool to inhibit the activation of NF-κB.[88] These findings collectively justify the normalization of the elevated iNOS and TNF-α levels induced after exposure to IMI.

5. CONCLUSIONS

Our findings revealed that IMI is highly neurotoxic to nontarget organisms and exerts its toxic action via oxidative stress that mediates the mechanistic way of cellular apoptosis and inflammation. Both *O. majorana* oil and methanol extract have strong antioxidant, anti-inflammatory, and anti-apoptotic properties, besides their neurotransmitters' modulatory role, which can effectively protect against IMI neurotoxicity. We suggest using Origanum to safeguard against the neuroinflammation and oxidative stress induced by insecticide exposure. The current study could help assess the risks of neonicotinoid use to nontarget organisms, but there are major knowledge gaps about its pharmacokinetics and pharmacodynamics. A deeper analysis should concentrate on minimizing the side effects of extensive insecticide use and their leakage into the surrounding environment. Furthermore, searching for new alternatives to the current insecticides with less hazardous effects on the surrounding environment is very important in the future.

ASSOCIATED CONTENT

Data Availability Statement

All data are available on request.

AUTHOR INFORMATION

Corresponding Author

Sherif Ashraf Fahmy − *Department of Chemistry, School of Life and Medical Sciences, University of Hertfordshire Hosted by Global Academic Foundation, 11835 Cairo, Egypt;* orcid.org/0000-0003-3056-8281; Phone: +20 1222613344; Email: s.fahmy@herts.ac.uk, sheriffahmy@aucegypt.edu

Authors

Eman I. Hassanen − *Department of Pathology, Faculty of Veterinary Medicine, Cairo University, 12211 Giza, Egypt*

Marwa Y. Issa − *Department of Pharmacognosy, Faculty of Pharmacy, Cairo University, 11562 Cairo, Egypt*

Neven H. Hassan − *Department of Physiology, Faculty of Veterinary Medicine, Cairo University, 12211 Giza, Egypt*

Marwa A. Ibrahim − *Department of Biochemistry, Faculty of Veterinary Medicine, Cairo University, 12211 Giza, Egypt*

Iten M. Fawzy − *Department of Pharmaceutical Chemistry, Faculty of Pharmacy, Future University in Egypt, 11835 Cairo, Egypt*

Sally Mehanna − *Department of Animal Hygiene and Management, Faculty of Veterinary Medicine, Cairo University, 12211 Giza, Egypt*

Complete contact information is available at: https://pubs.acs.org/10.1021/acsomega.2c08295

Funding

This research has not received any specific grant from public, commercial, or not-for-profit funding agencies.

Notes

The authors declare no competing financial interest.
All Institutional and National Guidelines for the care and use of animals were followed.

REFERENCES

(1) Abu Zeid, E. H.; Alam, R. T. M.; Ali, S. A.; Hendawi, M. Y. Dose-related impacts of imidacloprid oral intoxication on brain and liver of rock pigeon (Columba livia domestica), residues analysis in different organs. *Ecotoxicol. Environ. Saf.* **2019**, *167*, 60−68.

(2) Jeschke, P.; Nauen, R.; Schindler, M.; Elbert, A. Overview of the Status and Global Strategy for Neonicotinoids. *J. Agric. Food Chem.* **2011**, *59*, 2897−2908.

(3) Gibbons, D.; Morrissey, C.; Mineau, P. A review of the direct and indirect effects of neonicotinoids and fipronil on vertebrate wildlife. *Environ. Sci. Pollut. Res.* **2015**, *22*, 103−118.

(4) Cimino, A. M.; Boyles, A. L.; Thayer, K. A.; Perry, M. J. Effects of Neonicotinoid Pesticide Exposure on Human Health: A Systematic Review. *Environ. Health Perspect.* **2017**, *125*, 155−162.

(5) Han, W.; Tian, Y.; Shen, X. Human exposure to neonicotinoid insecticides and the evaluation of their potential toxicity: An overview. *Chemosphere* **2018**, *192*, 59−65.

(6) Katić, A.; Kašuba, V.; Kopjar, N.; Lovaković, B. T.; Marjanović Čermak, A. M.; Mendaš, G.; Micek, V.; Milić, M.; Pavičić, I.; Pizent, A.; Žunec, S.; Želježić, D. Effects of low-level imidacloprid oral exposure on cholinesterase activity, oxidative stress responses, and

https://doi.org/10.1021/acsomega.2c08295
ACS Omega 2023, 8, 18491−18508

primary DNA damage in the blood and brain of male Wistar rats. *Chem. Biol. Interact.* **2021**, *338*, No. 109287.
(7) Mikolić, A.; Karačonji, I. B. Imidacloprid as reproductive toxicant and endocrine disruptor: investigations in laboratory animals. *Arch. Ind. Hyg. Toxicol.* **2018**, *69*, 103−108.
(8) Lonare, M.; Kumar, M.; Raut, S.; Badgujar, P.; Doltade, S.; Telang, A. Evaluation of imidacloprid-induced neurotoxicity in male rats: A protective effect of curcumin. *Neurochem. Int.* **2014**, *78*, 122−129.
(9) Coccimiglio, J.; Alipour, M.; Jiang, Z.-H.; Gottardo, C.; Suntres, Z. Antioxidant, Antibacterial, and Cytotoxic Activities of the Ethanolic Origanum vulgare Extract and Its Major Constituents. *Oxid. Med. Cell. Longevity* **2016**, *2016*, No. 1404505.
(10) Yu, M.; Gouvinhas, I.; Rocha, J.; Barros, A. I. Phytochemical and antioxidant analysis of medicinal and food plants towards bioactive food and pharmaceutical resources. *Sci. Rep.* **2021**, *11*, No. 10041.
(11) Sakkas, H.; Papadopoulou, C. Antimicrobial Activity of Basil, Oregano, and Thyme Essential Oils. *J. Microbiol. Biotechnol.* **2017**, *27*, 429−438.
(12) Davidenco, V.; Argüello, J. A.; Piccardi, M. B.; Vega, C. R. C. Day length modulates precocity and productivity through its effect on developmental rate in Origanum vulgare ssp. *Sci. Hortic.* **2017**, *218*, 164−170.
(13) Loizzo, M. R.; Menichini, F.; Conforti, F.; Tundis, R.; Bonesi, M.; Saab, A. M.; Statti, G. A.; de Cindio, B.; Houghton, P. J.; Menichini, F.; Frega, N. G. Chemical analysis, antioxidant, anti-inflammatory and anticholinesterase activities of Origanum ehrenbergii Boiss and Origanum syriacum L. essential oils. *Food Chem.* **2009**, *117*, 174−180.
(14) Chishti, S.; Kaloo, Z. A. Medicinal importance of genus Origanum: A review. *J. Pharmacogn. Phyther.* **2013**, *5*, 170−177.
(15) Henning, S. M.; Zhang, Y.; Seeram, N. P.; Lee, R.-P.; Wang, P.; Bowerman, S.; Heber, D. Antioxidant capacity and phytochemical content of herbs and spices in dry, fresh and blended herb paste form. *Int. J. Food Sci. Nutr.* **2011**, *62*, 219−225.
(16) Leyva-López, N.; Gutiérrez-Grijalva, E.; Vazquez-Olivo, G.; Heredia, J. Essential Oils of Oregano: Biological Activity beyond Their Antimicrobial Properties. *Molecules* **2017**, *22*, 989.
(17) Issa, M. Y.; Ezzat, M. I.; Sayed, R. H.; Elbaz, E. M.; Omar, F. A.; Mohsen, E. Neuroprotective effects of Pulicaria undulata essential oil in rotenone model of Parkinson's disease in rats: Insights into its anti-inflammatory and antioxidant effects. *S. Afr. J. Bot.* **2020**, *132*, 289−298.
(18) Ali, S. E.; El Badawy, S. A.; Elmosalamy, S. H.; Emam, S. R.; Azouz, A. A.; Galal, M. K.; Abd-Elsalam, R. M.; Issa, M. Y.; Hassan, B. B. Novel promising reproductive and metabolic effects of Cicer arietinum L. extract on letrozole induced polycystic ovary syndrome in rat model. *J. Ethnopharmacol.* **2021**, *278*, No. 114318.
(19) Hassanen, E. I.; Hussien, A. M.; Mehanna, S.; Ibrahim, M. A.; Hassan, N. H. Comparative assessment on the probable mechanisms underlying the hepatorenal toxicity of commercial imidacloprid and hexaflumuron formulations in rats. *Environ. Sci. Pollut. Res.* **2022**, *29*, 29091−29104.
(20) Pimple, B. P.; Kadam, P. V.; Patil, M. J. Comparative antihyperglycaemic and antihyperlipidemic effect of *Origanum majorana* extracts in NIDDM rats. *Orient. Pharm. Exp. Med.* **2012**, *12*, 41−50.
(21) Selvarasu, K.; Singh, A. K.; Iyaswamy, A.; Gopalkrishnashetty Sreenivasmurthy, S.; Krishnamoorthi, S.; Bera, A. K.; Huang, J. D.; Durairajan, S. S. K. Reduction of kinesin I heavy chain decreases tau hyperphosphorylation, aggregation, and memory impairment in Alzheimer's disease and tauopathy models. *Front. Mol. Biosci.* **2022**, *9*, 1179.
(22) Can, A.; Dao, D. T.; Arad, M.; Terrillion, C. E.; Piantadosi, S. C.; Gould, T. D. The Mouse Forced Swim Test. *J. Visualized Exp.* **2012**, *59*, No. 3638.
(23) Yankelevitch-Yahav, R.; Franko, M.; Huly, A.; Doron, R. The Forced Swim Test as a Model of Depressive-like Behavior. *J. Visualized Exp.* **2015**, *97*, No. 52587.
(24) Sreenivasmurthy, S. G.; Ashok, I.; Krishnamoorthi, S.; Reddi, R.; Kammala, A. K.; Vasudevan, K.; Senapati, S.; Zhu, Z.; SU, C.; Liu, J.; Guan, X. J.; et al. Bromo-protopine, a novel protopine derivative, alleviates tau pathology by activating chaperone-mediated autophagy for Alzheimer's disease therapy. *Front. Mol. Biosci.* **2022**, *9*, 1123.
(25) Hassanen, E. I.; Hussien, A. M.; Hassan, N. H.; Ibrahim, M. A.; Mehanna, S. A Comprehensive Study on the Mechanistic Way of Hexaflumuron and Hymexazol Induced Neurobehavioral Toxicity in Rats. *Neurochem. Res.* **2022**, *47*, 3051−3062.
(26) George, J.; Ellman, L.; Diane Courtney, K.; Valentino, A.; Featherstone, R. M. A new and rapid colorimetric determination of acetylcholine estrase activity. *Biochem. Pharmacol.* **1961**, *7*, 88−95.
(27) Gorun, V.; Proinov, I.; Bălţescu, V.; Balaban, G.; Bârzu, O. Modified Ellman procedure for assay of cholinesterases in crude enzymatic preparations. *Anal. Biochem.* **1978**, *86*, 324−326.
(28) Pagel, P.; Blome, J.; Wolf, H. U. High-performance liquid chromatographic separation and measurement of various biogenic compounds possibly involved in the pathomechanism of Parkinson's disease. *J. Chromatogr. B: Biomed. Sci. Appl.* **2000**, *15*, 297−304.
(29) Heinrikson, R. L.; Heinrikson, R. L. Amino acid analysis by reverse-phase high-performance liquid chromatography: precolumn derivatization with phenylisothiocyanate. *Anal. Biochem.* **1984**, *136*, 65−74.
(30) Noshy, P. A.; Elhady, M. A.; Khalaf, A. A. A.; Kamel, M. M.; Hassanen, E. I. Ameliorative effect of carvacrol against propiconazole-induced neurobehavioral toxicity in rats. *Neurotoxicology* **2018**, *67*, 141−149.
(31) Khalaf, A. A.; Hassanen, E. I.; Ibrahim, M. A.; Tohamy, A. F.; Aboseada, M. A.; Hassan, H. M.; Zaki, A. R. Rosmarinic acid attenuates chromium-induced hepatic and renal oxidative damage and DNA damage in rats. *J. Biochem. Mol. Toxicol.* **2020**, *34*, No. e22579.
(32) He, M. M.; Smith, A. S.; Oslob, J. D.; Flanagan, W. M.; Braisted, A. C.; Whitty, A.; Cancilla, M. T.; Wang, J.; Lugovskoy, A. A.; Yoburn, J. C.; Fung, A. D.; Farrington, G.; Eldredge, J. K.; Day, E. S.; Cruz, L. A.; Cachero, T. G.; Miller, S. K.; Friedman, J. E.; Choong, I. C.; Cunningham, B. C. Small-Molecule Inhibition of TNF-α. *Science* **2005**, *310*, 1022−1025.
(33) Davey, D. D.; Adler, M.; Arnaiz, D.; Eagen, K.; Erickson, S.; Guilford, W.; Kenrick, M.; Morrissey, M. M.; Ohlmeyer, M.; Pan, G.; Paradkar, V. M.; Parkinson, J.; Polokoff, M.; Saionz, K.; Santos, C.; Subramanyam, B.; Vergona, R.; Wei, R. G.; Whitlow, M.; Ye, B.; Zhao, Z.; Devlin, J. J.; Phillips, G. Design, Synthesis, and Activity of 2-Imidazol-1-ylpyrimidine Derived Inducible Nitric Oxide Synthase Dimerization Inhibitors. *J. Med. Chem.* **2007**, *50*, 1146−1157.
(34) Mehanna, S.; Issa, M. Y.; Hassan, N. H.; Hussien, A. M.; Ibrahim, M. A.; Hassanen, E. I. *Origanum majorana* essential oil improves the rat's sexual behavior and testicular oxidative damage induced by imidacloprid via modulating the steroidogenesis pathways. *Saudi Pharm. J.* **2022**, *30*, 1315−1326.
(35) Hossain, M. B.; Camphuis, G.; Aguiló-Aguayo, I.; Gangopadhyay, N.; Rai, D. K. Antioxidant activity guided separation of major polyphenols of marjoram (*Origanum majorana* L.) using flash chromatography and their identification by liquid chromatography coupled with electrospray ionization tandem mass spectrometry†. *J. Sep. Sci.* **2014**, *37*, 3205−3213.
(36) Taamalli, A.; Arráez-Román, D.; Abaza, L.; Iswaldi, I.; Fernández-Gutiérrez, A.; Zarrouk, M.; Segura-Carretero, A. LC-MS-based metabolite profiling of methanolic extracts from the medicinal and aromatic species Mentha pulegium and *Origanum majorana*. *Phytochem. Anal.* **2015**, *26*, 320−330.
(37) Li, J.; Wang, S.-P.; Wang, Y.-Q.; Shi, L.; Zhang, Z.-K.; Dong, F.; Li, H.-R.; Zhang, J.-Y.; Man, Y.-Q. Comparative metabolism study on chlorogenic acid, cryptochlorogenic acid and neochlorogenic acid using UHPLC-Q-TOF MS coupled with network pharmacology. *Chin. J. Nat. Med.* **2021**, *19*, 212−224.

https://doi.org/10.1021/acsomega.2c08295
ACS Omega 2023, 8, 18491−18508

(38) Chen, S.-D.; Lu, C.-J.; Zhao, R.-Z. Identification and Quantitative Characterization of PSORI-CM01, a Chinese Medicine Formula for Psoriasis Therapy, by Liquid Chromatography Coupled with an LTQ Orbitrap Mass Spectrometer. *Molecules* **2015**, *20*, 1594−1609.
(39) Kaiser, A.; Carle, R.; Kammerer, D. R. Effects of blanching on polyphenol stability of innovative paste-like parsley (Petroselinum crispum (Mill.) Nym ex A. W. Hill) and marjoram (*Origanum majorana* L.) products. *Food Chem.* **2013**, *138*, 1648−1656.
(40) Cao, J.-L.; Wang, S.-S.; Hu, H.; He, C.-W.; Wan, J.-B.; Su, H.-X.; Wang, Y.-T.; Li, P. Online comprehensive two-dimensional hydrophilic interaction chromatography × reversed-phase liquid chromatography coupled with hybrid linear ion trap Orbitrap mass spectrometry for the analysis of phenolic acids in Salvia miltiorrhiza. *J. Chromatogr. A* **2018**, *1536*, 216−227.
(41) Gürbüz, P.; Martinez, A.; Pérez, C.; Martínez-González, L.; Göger, F.; Ayran, İ. Potential anti-Alzheimer effects of selected Lamiaceae plants through polypharmacology on glycogen synthase kinase-3β, β-secretase, and casein kinase 1δ. *Ind. Crops Prod.* **2019**, *138*, No. 111431.
(42) Fecka, I.; Turek, S. Determination of polyphenolic compounds in commercial herbal drugs and spices from Lamiaceae: thyme, wild thyme and sweet marjoram by chromatographic techniques. *Food Chem.* **2008**, *108*, 1039−1053.
(43) Vujicic, M.; Nikolic, I.; Kontogianni, V. G.; Saksida, T.; Charisiadis, P.; Orescanin-Dusic, Z.; Blagojevic, D.; Stosic-Grujicic, S.; Tzakos, A. G.; Stojanovic, I. Methanolic extract of Origanum vulgare ameliorates type 1 diabetes through antioxidant, anti-inflammatory and anti-apoptotic activity. *Br. J. Nutr.* **2015**, *113*, 770−782.
(44) Gao, B.; Qin, F.; Ding, T.; Chen, Y.; Lu, W.; Yu, L. Differentiating Organically and Conventionally Grown Oregano Using Ultraperformance Liquid Chromatography Mass Spectrometry (UPLC-MS), Headspace Gas Chromatography with Flame Ionization Detection (Headspace-GC-FID), and Flow Injection Mass Spectrum (FIMS). *J. Agric. Food Chem.* **2014**, *62*, 8075−8084.
(45) Farag, M. A.; Ezzat, S. M.; Salama, M. M.; Tadros, M. G. Antiacetylcholinesterase potential and metabolome classification of 4 Ocimum species as determined via UPLC/qTOF/MS and chemometric tools. *J. Pharm. Biomed. Anal.* **2016**, *125*, 292−302.
(46) Hossain, M. B.; Rai, D. K.; Brunton, N. P.; Martin-Diana, A. B.; Barry-Ryan, C. Characterization of Phenolic Composition in Lamiaceae Spices by LC-ESI-MS/MS. *J. Agric. Food Chem.* **2010**, *58*, 10576−10581.
(47) Velamuri, R.; Sharma, Y.; Fagan, J.; Schaefer, J. Application of UHPLC-ESI-QTOF-MS in Phytochemical Profiling of Sage (Salvia officinalis) and Rosemary (Rosmarinus officinalis). *Planta Medica Int. Open* **2020**, *7*, e133−e144.
(48) Emam, S. R.; Abd-Elsalam, R. M.; Azouz, A. A.; Ali, S. E.; El Badawy, S. A.; Ibrahim, M. A.; Hassan, B. B.; Issa, M. Y.; Elmosalamy, S. H. Linum usitatissimum seeds oil down-regulates mRNA expression for the steroidogenic acute regulatory protein and Cyp11A1 genes, ameliorating letrezole-induced polycystic ovarian syndrome in a rat model. *J. Physiol. Pharmacol.* **2021**, *72*, 55−67.
(49) Shen, D.; Pan, M.-H.; Wu, Q.-L.; Park, C.-H.; Juliani, H. R.; Ho, C.-T.; Simon, J. E. LC-MS Method for the Simultaneous Quantitation of the Anti-inflammatory Constituents in Oregano (Origanum Species). *J. Agric. Food Chem.* **2010**, *58*, 7119−7125.
(50) Hassanen, E. I.; Ibrahim, M. A.; Hassan, A. M.; Mehanna, S.; Aljuaydi, S. H.; Issa, M. Y. Neuropathological and Cognitive Effects Induced by CuO-NPs in Rats and Trials for Prevention Using Pomegranate Juice. *Neurochem. Res.* **2021**, *46*, 1264−1279.
(51) El-lethey, H. S.; Kamel, M. M. Effects of black tea in mitigation of sodium fluoride potency to suppress motor activity and coordination in laboratory rats. *J. Am. Sci.* **2011**, *7*, 243−254.
(52) Weisstaub, N. V.; Zhou, M.; Lira, A.; Lambe, E.; González-Maeso, J.; Hornung, J.-P.; Sibille, E.; Underwood, M.; Itohara, S.; Dauer, W. T.; Ansorge, M. S.; Morelli, E.; Mann, J. J.; Toth, M.; Aghajanian, G.; Sealfon, S. C.; Hen, R.; Gingrich, J. A. Cortical 5-HT 2A Receptor Signaling Modulates Anxiety-Like Behaviors in Mice. *Science* **2006**, *313*, 536−540.
(53) Anderson, N. L.; Hughes, R. N. Increased emotional reactivity in rats following exposure to caffeine during adolescence. *Neurotoxicol. Teratol.* **2008**, *30*, 195−201.
(54) Fromm, L.; Heath, D. L.; Vink, R.; Nimmo, A. J. Magnesium Attenuates Post-Traumatic Depression/Anxiety Following Diffuse Traumatic Brain Injury in Rats. *J. Am. Coll. Nutr.* **2004**, *23*, 529S−533S.
(55) Elhady, M. A.; Khalaf, A. A. A.; Kamel, M. M.; Noshy, P. A. Carvacrol ameliorates behavioral disturbances and DNA damage in the brain of rats exposed to propiconazole. *Neurotoxicology* **2019**, *70*, 19−25.
(56) Najjar, F.; Ahmad, M.; Lagace, D.; Leenen, F. H. H. Sex differences in depression-like behavior and neuroinflammation in rats post-MI: role of estrogens. *Am. J. Physiol.: Heart Circ. Physiol.* **2018**, *315*, H1159−H1173.
(57) Abd-Elhakim, Y. M.; Mohammed, H. H.; Mohamed, W. A. Mohamed, Imidacloprid Impacts on Neurobehavioral Performance, Oxidative Stress, and Apoptotic Events in the Brain of Adolescent and Adult Rats. *J. Agric. Food Chem.* **2018**, *66*, 13513−13524.
(58) Hassanen, E. I.; Ebedy, Y. A.; Ibrahim, M. A.; Farroh, K. Y.; Elshazly, M. O. Insights overview on the possible protective effect of chitosan nanoparticles encapsulation against neurotoxicity induced by carbendazim in rats. *Neurotoxicology* **2022**, *91*, 31−43.
(59) Ognibene, E.; Middei, S.; Daniele, S.; Adriani, W.; Ghirardi, O.; Caprioli, A.; Laviola, G. Aspects of spatial memory and behavioral disinhibition in Tg2576 transgenic mice as a model of Alzheimer's disease. *Behav. Brain Res.* **2005**, *156*, 225−232.
(60) Wolf, A.; Bauer, B.; Abner, E. L.; Ashkenazy-Frolinger, T.; Hartz, A. M. S. A Comprehensive Behavioral Test Battery to Assess Learning and Memory in 129S6/Tg2576 Mice. *PLoS One* **2016**, *11*, No. e0147733.
(61) Kara, M.; Yumrutas, O.; Demir, C. F.; Ozdemir, H. H.; Bozgeyik, I.; Coskun, S.; Eraslan, E.; Bal, R. Insecticide imidacloprid influences cognitive functions and alters learning performance and related gene expression in a rat model. *Int. J. Exp. Pathol.* **2015**, *96*, 332−337.
(62) Abd-Elhakim, Y. M.; Mohammed, H. H.; Mohamed, W. A. M. Imidacloprid Impacts on Neurobehavioral Performance, Oxidative Stress, and Apoptotic Events in the Brain of Adolescent and Adult Rats. *J. Agric. Food Chem.* **2018**, *66*, 13513−13524.
(63) Rawi, S. M.; Al-Logmani, A. S.; Hamza, R. Z. Neurological alterations induced by formulated imidacloprid toxicity in Japanese quails. *Metab. Brain Dis.* **2019**, *34*, 443−450.
(64) Salim, S. Oxidative Stress and the Central Nervous System. *J. Pharmacol. Exp. Ther.* **2017**, *360*, 201−205.
(65) Duzguner, V.; Erdogan, S. Chronic exposure to imidacloprid induces inflammation and oxidative stress in the liver and central nervous system of rats. *Pestic. Biochem. Physiol.* **2012**, *104*, 58−64.
(66) Hassanen, E. I.; Kamel, S.; Mohamed, W. A.; Mansour, H. A.; Mahmoud, M. A. The potential mechanism of histamine-inducing cardiopulmonary inflammation and apoptosis in a novel oral model of rat intoxication. *Toxicology* **2023**, *484*, No. 153410.
(67) Poon, H. F.; Vaishnav, R. A.; Getchell, T. V.; Getchell, M. L.; Butterfield, D. A. Quantitative proteomics analysis of differential protein expression and oxidative modification of specific proteins in the brains of old mice. *Neurobiol. Aging* **2005**, *27*, 1110−1119.
(68) Gasmi, S.; Chafaa, S.; Lakroun, Z.; Rouabhi, R.; Touahria, C.; Kebieche, M.; Soulimani, R. Neuronal Apoptosis and Imbalance of Neurotransmitters Induced by Acetamiprid in Rats. *Toxicol. Environ. Health Sci.* **2019**, *11*, 305−311.
(69) Bhardwaj, S.; Srivastava, M. K.; Kapoor, U.; Srivastava, L. P. A 90 days oral toxicity of imidacloprid in female rats: Morphological, biochemical and histopathological evaluations. *Food Chem. Toxicol.* **2010**, *48*, 1185−1190.
(70) Vohra, P.; Khera, K. S.; Sangha, G. K. Physiological, biochemical and histological alterations induced by administration

https://doi.org/10.1021/acsomega.2c08295
ACS Omega 2023, 8, 18491−18508

of imidacloprid in female albino rats. *Pestic. Biochem. Physiol.* **2014**, *110*, 50−56.
(71) Ebedy, Y. A.; Hassanen, E. I.; Hussien, A. M.; Ibrahim, M. A.; Elshazly, M. O. Neurobehavioral Toxicity Induced by Carbendazim in Rats and the Role of iNOS, Cox-2, and NF-κB Signalling Pathway. *Neurochem. Res.* **2022**, *47*, 1956−1971.
(72) Mo, E.; Ebedy, Y. A.; Ibrahim, M. A.; Farroh, K. Y.; Hassanen, E. I. Newly synthesized chitosan-nanoparticles attenuate carbendazim hepatorenal toxicity in rats via activation of Nrf2/HO1 signalling pathway. *Sci. Rep.* **2022**, *12*, No. 9986.
(73) Hassan, N. H.; Mehanna, S.; Hussien, A. M.; Ibrahim, M. A.; Hassanen, E. I. The potential mechanism underlying the hepatorenal toxicity induced by hymexazol in rats and the role of NF-κB signaling pathway. *J. Biochem. Mol. Toxicol.* **2023**, *37*, No. e23304.
(74) Hassanen, E. I.; Tohamy, A.; Issa, M. Y.; Ibrahim, M. A.; Farroh, K. Y.; Hassan, A. M. Pomegranate Juice Diminishes The Mitochondria-Dependent Cell Death And NF-kB Signaling Pathway Induced By Copper Oxide Nanoparticles On Liver And Kidneys Of Rats. *Int. J. Nanomedicine* **2019**, *14*, 8905−8922.
(75) Postu, P. A.; Gorgan, D. L.; Cioanca, O.; Russ, M.; Mikkat, S.; Glocker, M. O.; Hritcu, L. Memory-Enhancing Effects of *Origanum majorana* Essential Oil in an Alzheimer's Amyloid beta1-42 Rat Model: A Molecular and Behavioral Study. *Antioxidants* **2020**, *9*, 919.
(76) Vági, E.; Rapavi, E.; Hadolin, M.; Vásárhelyiné Perédi, K.; Balázs, A.; Blázovics, A.; Simándi, B. Phenolic and Triterpenoid Antioxidants from *Origanum majorana* L. Herb and Extracts Obtained with Different Solvents. *J. Agric. Food Chem.* **2005**, *53*, 17−21.
(77) Abbasi-Maleki, S.; Kadkhoda, Z.; Taghizad-Farid, R. The antidepressant-like effects of *Origanum majorana* essential oil on mice through monoaminergic modulation using the forced swimming test. *J. Tradit. Complementary Med.* **2020**, *10*, 327−335.
(78) Amaghnouje, A.; Mechchate, H.; Es-safi, I.; Alotaibi, A. A.; Noman, O. M.; Nasr, F. A.; Al-zharani, M.; Cerruti, P.; Calarco, A.; Fatemi, H. E. L.; Grafov, A.; Bousta, D. Anxiolytic, Antidepressant-Like Proprieties and Impact on the Memory of the Hydro-Ethanolic Extract of *Origanum majorana* L. on Mice. *Appl. Sci.* **2020**, *10*, 8420.
(79) Mombeini, T.; Mazloumi, S.; Shams, J. Pharmacological Effects of *Origanum vulgare* L. in the Elevated Plus-Maze and Open Field Tests in the Rat. *J. Basic Clin. Pathophysiol.* **2015**, *3*, 29−36.
(80) Amiresmaeili, A.; Roohollahi, S.; Mostafavi, A.; Askari, N. Effects of oregano essential oil on brain TLR4 and TLR2 gene expression and depressive-like behavior in a rat model. *Res. Pharm. Sci.* **2018**, *13*, 130.
(81) Postu, P. A.; Gorgan, D. L.; Cioanca, O.; Russ, M.; Mikkat, S.; Glocker, M. O.; Hritcu, L. Memory-Enhancing Effects of *Origanum majorana* Essential Oil in an Alzheimer's Amyloid beta1−42 Rat Model: A Molecular and Behavioral Study. *Antioxidants* **2020**, *9*, 919.
(82) Mossa, A. T. H.; Nawwar, G. Free radical scavenging and antiacetylcholinesterase activities of *Origanum majorana* L. essential oil. *Hum. Exp. Toxicol.* **2011**, *30*, 1501−1513.
(83) Hajlaoui, H.; Mighri, H.; Aouni, M.; Gharsallah, N.; Kadri, A. Chemical composition and in vitro evaluation of antioxidant, antimicrobial, cytotoxicity and antiacetylcholinesterase properties of Tunisian *Origanum majorana* L. essential oil. *Microb. Pathog.* **2016**, *95*, 86−94.
(84) Duletić-Laušević, S.; Aradski, A. A.; Kolarević, S.; Vuković-Gačić, B.; Oalde, M.; Živković, J.; Šavikin, K.; Marin, P. D. Antineurodegenerative, antioxidant and antibacterial activities and phenolic components of *Origanum majorana* L. (Lamiaceae) extracts. *J. Appl. Bot. Food Qual.* **2018**, *91*, 126−134.
(85) Deshmane, D. N.; Gadgoli, C. H.; Halade, G. V. Anticonvulsant effect of *Origanum majorana* L. *Pharmacologyonline* **2007**, *1*, 64−78.
(86) Olmos, G.; Lladó, J. Tumor Necrosis Factor Alpha: A Link between Neuroinflammation and Excitotoxicity. *Mediators Inflammation* **2014**, *2014*, No. 861231.
(87) Rahbardar, M. G.; Amin, B.; Mehri, S.; Mirnajafi-Zadeh, S. J.; Hosseinzadeh, H. Rosmarinic acid attenuates development and existing pain in a rat model of neuropathic pain: An evidence of anti-oxidative and anti-inflammatory effects. *Phytomedicine* **2018**, *40*, 59−67.
(88) Li, J.; Zhang, X.; Huang, H. Protective effect of linalool against lipopolysaccharide/d-galactosamine-induced liver injury in mice. *Int. Immunopharmacol.* **2014**, *23*, 523−529.

https://doi.org/10.1021/acsomega.2c08295
ACS Omega 2023, 8, 18491−18508